DOCTORAL THESIS

Cytotoxic dynamics of natural killer cell at the single cell level

Zhu, Yanting

Date of Award:
2018

HONG KONG BAPTIST UNIVERSITY

Doctor of Philosophy

THESIS ACCEPTANCE

DATE: September 5, 2018

STUDENT'S NAME: ZHU Yanting

THESIS TITLE: Cytotoxic Dynamics of Natural Killer Cell at the Single Cell Level

This is to certify that the above student's thesis has been examined by the following panel members and has received full approval for acceptance in partial fulfillment of the requirements for the degree of Doctor of Philosophy.

Chairman:	Dr Tong Tiejun Associate Professor, Department of Mathematics, HKBU (Designated by Dean of Faculty of Science)
Internal Members:	Prof Van Hove M. A. Chair Professor, Department of Physics, HKBU
	Prof Mak Nai Ki Professor, Department of Biology, HKBU
External Members:	Prof Wong Alice Sze-Tsai Associate Professor School of Biological Sciences The University of Hong Kong
	Dr Lam Yun Wah Associate Professor Department of Biology and Chemistry City University of Hong Kong
In-attendance:	Dr Shi Jue Associate Professor, Department of Physics, HKBU

Issued by Graduate School, HKBU

Cytotoxic Dynamics of Natural Killer Cell at the Single Cell Level

ZHU Yanting

A thesis submitted in partial fulfillment of the requirements

for the degree of

Doctor of Philosophy

Principal Supervisor: Dr. SHI Jue

Hong Kong Baptist University

August 2018

DECLARATION

I hereby declare that this thesis represents my own work, which has been done after registration for the degree of PhD at Hong Kong Baptist University and has not been previously included in a thesis or dissertation submitted to this or any other institution for a degree, diploma or other qualifications.

I have read the University's current research ethics guidelines, and accept responsibility for the conduct of the procedures in accordance with the University's Committee on the Use of Human & Animal Subjects in Teaching and Research (HASC). I have attempted to identify all the risks related to this research that may arise in conducting this research, obtained the relevant ethical and/or safety approval (where applicable), and acknowledged my obligations and the rights of the participants.

Signature: 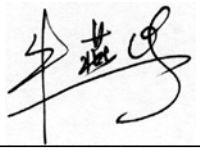

Date: August 2018

Abstract

Natural Killer (NK) cell, a crucial player of the human innate immune defense system, detects and kills virus-infected cells and cancer cells. Although the relevant molecular machineries involved in NK cell activation and NK-target cell interactions are largely known, how their collected dynamics regulate fast yet highly selective target cell killing in the complex environment of tissues is poorly understood. In traditional bulk killing assays, heterogeneity and kinetic details of individual NK-target cell interactions are masked, seriously limiting analysis of the underlying dynamic mechanisms. Therefore, the aim of my PhD study is to develop quantitative microscopy assays to elucidate, at the single cell level, real-time killing dynamics of epithelial cancer cells by primary NK cells purified from human blood. Results from my study not only identified the rate-limiting kinetics in NK-cancer cell interaction and mechanistically relevant heterogeneity in the process, but also characterized key molecular events and regulatory components of the NK cell machinery that were associated with the observed cytotoxic dynamics and heterogeneity. NK cells are considered promising candidate for cancer treatment, especially for eliminating residual cancer cells after conventional therapy. The fundamental knowledge acquired from my PhD study, in particular regarding how killing by primary NK cell varies between different target cancer cell types, provides new mechanistic insight that may help to develop this treatment strategy. And the quantitative microscopy assays that I developed are readily extendable to analysis of other cell-cell interaction dynamics, e.g., involved in cytotoxic T cell function.

Acknowledgements

Foremost, I would like to express my deepest appreciation to my supervisor Dr. SHI Jue. Her continuous guidance and encouragement helped me throughout my research project and writing of this thesis. Her motivation, enthusiasm and patience affected me a lot, and her inspiring ideas, keen academic observation, and rigorous attitude enlightened me.

I am very grateful for the advice and technical support form Prof. PANG, Stella W., Dr. Y W LAM and lab mates in their laboratory at the City University of Hong Kong, for engineering microfluidic chips which was applied in NK-cancer cell imaging.

I would like to extend my thanks to Ms. Cheng Sau Kuen for technical support and kind assistance. I am thankful to my colleagues, Dr. ZHOU Yuan, Ms. CHEN Xi, and Dr. HUANG Bo, for their help and advice. Special thanks also go to my friends YU Xiao and ZHANG Wei for our friendship.

Last but not least, I take this opportunity to express profound gratitude from my heart to my Mom. Thank you so much for everything you have done for me.

Contents

DECLARATION i

Abstract ii

Acknowledgements iii

Contents iv

List of Tables and Figures vi

Chapter 1 Introduction 1

1.1 Basic characteristics of Natural Killer (NK) cell 1

1.2 Target recognition by NK cell through activating and inhibitory receptors 3

1.3 Major cytotoxic mechanisms of NK cell 7

1.4 NK cell activity against virus-infected and cancer targets 10

1.5 Cancer immunotherapy 12

1.6 Objective of the study 17

Chapter 2 Research Methodology 18

2.1 Isolation of primary NK cells from human blood 18

2.2 Cell line and cell culture 19

2.3 Generation of fluorescent reporter cell lines and isogenic clones 20

2.4 Chemicals, siRNA oligo and neutralizing antibodies 21

2.5 Time-lapse microscopy and image analysis 21

2.6 Flow cytometry 22

Chapter 3 Quantitative characteristics of cytotoxic dynamics of primary human NK cell at the single cell level 24

3.1 Cytotoxic dynamics of primary human NK cell are distinct from cultured NK cell line, NK92-MI 24

3.2 Granzyme-B independent cytotoxicity of primary NK cell is mainly mediated by Fas ligand 30

3.3 Gradual caspase-8 induction triggered by transient FasL binding versus switch-like granzyme-B activation upon lytic granule transfer 33

3.4 Interleukin 2 promotes cancer target detection by NK cell and increases NK-target cell interaction 38

Chapter 4 Target specificity of cytotoxic dynamics of primary human NK cell 41

4.1 Cytotoxic mode and kinetics of primary NK cell depended on target cell type 41

4.2 Mechanism of necrotic death induced by primary NK cell 46

4.3 Target specificity of NK cell cytotoxic activity on inhibitory and activating NK cell receptors 50

4.4 Differential expression of activating and inhibitory ligands on target cells 55

Chapter 5 Discussion and Conclusion 58

References 69

List of Publications 84

CURRICULUM VITAE 85

List of Tables and Figures

Table 1.1. Expression level of surface markers of NK cells and other immune cell types showed differences (data taken from reference 1)……...2

Figure 1.1. Competing inhibitory and activating signaling that the NK cell receives through conjugation of various classes of NK cell receptors and their interacting ligands on target cell surface (figure taken from reference 49)…...…….....5

Table 1.2. Surface receptors of human NK cells and their respective interacting ligands on target cell (data taken from reference 46 and 47)……...……..6

Figure 1.2. Major cytotoxic mechanisms and functions of NK cell (figure taken from reference 51)….....9

Figure 1.3. Summary and classification of current approaches to cancer immunotherapy ……....14

Table 1.3. Overview of immune checkpoint molecules expressed on NK cells: pattern of expression, ligands, and impact on NK cell functions (table taken from reference 105)…….16

Figure 3.1. Cytotoxic dynamics of primary NK cells are distinct from NK cell line, NK92-MI……..……...28

Figure 3.2. Granzyme-B independent killing by primary NK cells is mainly mediated by extrinsic apoptosis induced by FasL……...32

Figure 3.3. The FasL and lytic granule cytotoxic pathways exhibited distinct activation kinetics and involved different types of NK-target cell conjugation…….36

Figure 3.4. IL-2 regulates the directionality of NK cell movement towards the target cell and the frequency of NK-target cell contact…….40

Figure 4.1. Characteristics of cytotoxic dynamics of primary NK cell against five different target cell lines……44

Figure 4.2. Necrotic death induced by primary NK cells is likely due to large membrane pores formed by perforin……48

Figure 4.3. Blocking inhibitory and activating receptors of primary NK cells showed differential effect on altering cell death response of the five target cell lines…….53

Figure 4.4. The five target cell lines expressed variable levels of NK cell activating and inhibitory ligands as well as Fas and integrin, ICAM-1, on cell surface……..57

Figure 5.1. Examples of PDMS chip design……..…….64

Chapter 1 Introduction

1.1 Basic characteristics of Natural Killer (NK) cell

Natural killer (NK) cell is large granular lymphocyte that can kill virus-infected cells and cancer cells without prior stimulation[1,2], thus belonging to the innate immune system. NK cells were first discovered in the 1970s in mice[3–7]. Based on its morphology, expression of lymphoid surface markers and origin from lymphoid progenitor cells, NK cell was subsequently classified as lymphocytes[1,5,6,8]. Early studies of NK cell already showed it can spontaneously exert selective and rapid cytolytic activity towards certain cancer cells without involvement of antibody activity[5,6]. Given such unique functional characteristics and the largely lack of surface makers similar to B and T lymphocyte, NK cell was later defined as a new subset of lymphocytes[5–7]. NK cell was present in many mammals, including human, rat and horse[9–21]. Although there are specie-specific differences in the characteristics of NK cell, and also disagreement on whether NK cell is yet another type of T cell, most findings in the literature support NK cell is a unique subset of lymphocyte because of its ability to eliminate abnormal cells in the absence of antibody or stimulation by other innate immune cell types[3–7,9–17,22].

NK cells comprise about 5% to 15% of the human peripheral blood lymphocytes (PBL)[23–26]. NK cells are also distributed in peripheral tissues and organs, including the lung, liver, spleen, bone marrow, lymph node, thymus and uterus (during pregnancy)[23,24,27–29]. NK cell expresses a number of characteristic surface makers, which are summarized in Table 1.1 based on the review by Robertson and Ritz[1]. However, most

of these surface markers are also expressed by other immune cell types. Therefore, there are inherent limitations in using any surface marker alone to identify or purify NK cell. In a typical cell sorting protocol to purify the NK cell population from blood sample, granulocytes, including basophil, eosinophil and neutrophil, are first separated from lymphocytes and monocytes by density gradient centrifugation. Then, by flow cytometry and with the lymphocyte gating on forward scattering (FSC) and side scattering (SSC) features, the monocytes are excluded[30–32]. And finally the absence of CD3 on NK cells separates the NK cell population from T cells. Given that most NK cells express CD56, NK cells are defined and identified phenotypically as $CD56^+$ $CD3^-$ lymphocytes[1,30,31,33].

Table 1.1. Expression level of surface markers of NK cells and other immune cell types showed differences (data taken from reference 1).

		NK cells	T cells	Monocytes	Neutrophils
Surface Markers	CD2	70-90%	>95%	<5%	<5%
	CD3	0%	>95%	0%	0%
	CD8	30-40%	30-40%	<5%	<5%
	CD11b	80-90%	10-15%	>90%	>90%
	CD15	<5%	<5%	60-80%	>95%
	CD16	80-90%	<5%	10-15%	>95%
	CD56	>95%	<5%	<5%	<5%

NK cells can be further divided into two subsets based on surface expression levels of CD16 and CD56, namely $CD16_{bright}CD56_{dim}$ and $CD16_{dim}CD56_{bright}$[31,34–36]. The

$CD16_{bright}CD56_{dim}$ NK cell subset accounts for 90% of the circulating human NK cells in the blood, while the $CD16_{dim}CD56_{bright}$ subset accounts for the other 10%[34–37]. However, almost 100% of NK cells found in the secondary lymphoid tissue belong to the $CD16_{dim}CD56_{bright}$ subset. The change of CD56 expression level from $CD56_{bright}$ in the circulating blood to $CD56_{dim}$ in tissue is likely a continuous process in NK cell development[31,38,39]. Moreover, the two subsets of NK cells are known to have distinct functions. Specifically, the $CD16_{bright}CD56_{dim}$ NK cells have high cytolytic capacity, thus playing the main cytotoxic role in recognizing and eliminating abnormal cells[35,36,39–41]. Meanwhile, the $CD16_{dim}CD56_{bright}$ subset act mainly as immuno-modulating cells to secrete inflammatory cytokines, such as IFN-γ and TNF-α, which subsequently activate other immune cell types towards a global immune response[34,36–42].

1.2 Target recognition by NK cell through activating and inhibitory receptors

NK cell activity against abnormal targets is mainly regulated by collective signaling transmitted by the competing activating and inhibitory receptors on NK cell surface. Every NK cell expresses a series of activating receptors, which recognize distinct ligands on virus-infected and cancer cells, as well as various inhibitory receptors, which recognize MHC class I (MHCI) molecules expressed by all nucleated cells[43]. Under non-stimulated conditions, the inhibitory receptors on NK cell surface prevent NK cells from killing the normal cells by interacting with their MHCI molecules. Upon binding to the activating ligands on abnormal cells, signaling from the activating receptors on NK cell outweighs the inhibitory signaling, thus activating the cytotoxic activity of NK cell towards the desired target[43–45]. In general, the overall balance of activating and inhibitory

signaling determines the extent of NK cell response and the outcome of NK-target cell interaction (Fig. 1.1 and Table 1.2)[46–49].

The major group of inhibitory receptors expressed by human NK cells that recognize classical MHCI molecules (i.e., HLA-A, -B and –C) are Killer cell Immunoglobulin-like Receptors (KIRs)[46]. And NKG2A (CD94/CD159a) is the other important NK cell inhibitory receptor that specifically engages non-classical MHCI molecule, HLA-E[46,47]. Reactivity of NK cell is believed to be calibrated by the self-MHCI molecule environment, and the number and/or strength of inhibitory receptor-MHCI interactions appeared to correlate with the effectiveness of abnormal cell elimination by NK cells. Compared to the small number of inhibitory receptors with a common inhibition mechanism, there is a much wider spectrum of NK cell activating receptors that trigger diverse signaling cascades, which probably evolve to respond to diverse aberrant ligands expressed by different virus-infected cells and transformed cells. The activating receptors of human NK cell can be roughly categorized into three subgroups based on their interacting partners, including: (1) those associated with immunoreceptor tyrosine-based activation motif (ITAM)-containing adaptor proteins; (2) those associated with non-ITAM; and (3) those associated with integrin[46]. Although the precise orchestration of signaling from the different inhibitory and activating receptors is still under investigation, it is generally accepted that collective activities of multiple NK cell receptors, rather than individual receptor-ligand interactions, is required to fully activate NK cell cytotoxic activity[46,48].

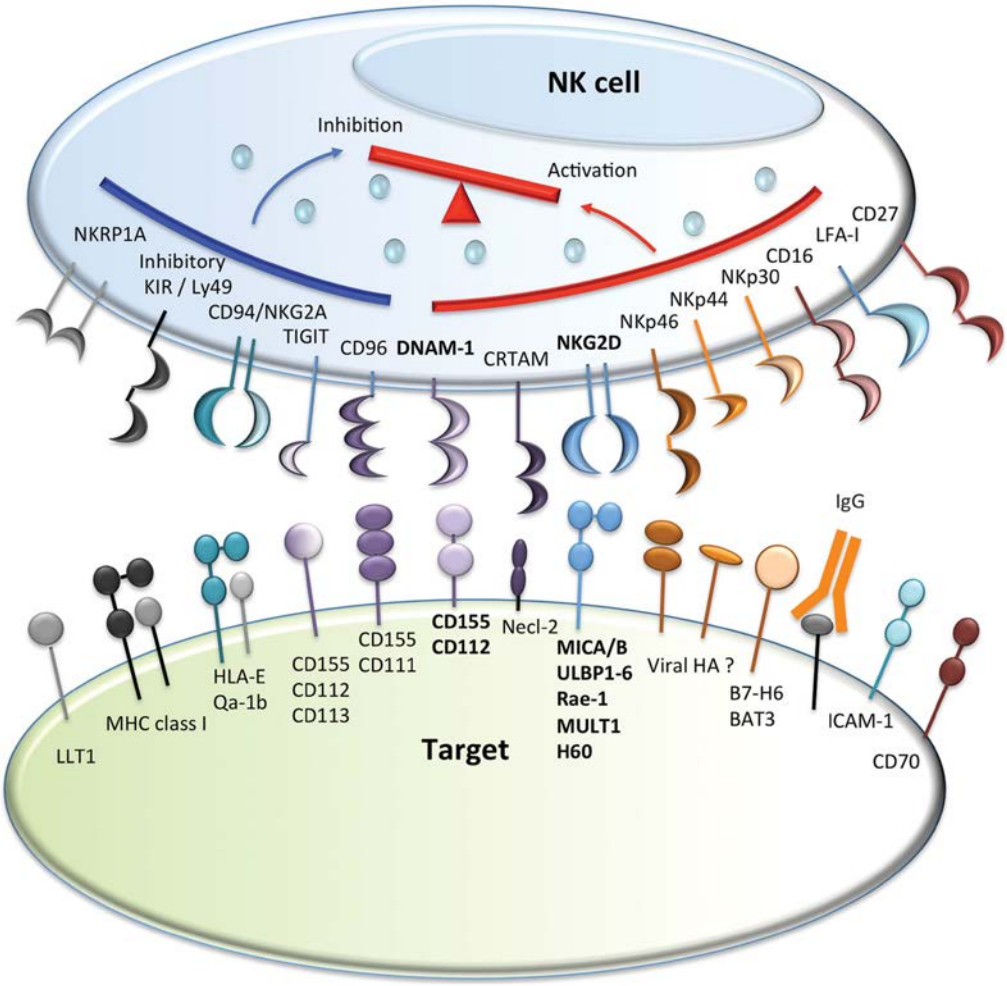

Figure 1.1. Competing inhibitory and activating signaling that the NK cell receives through conjugation of various classes of NK cell receptors and their interacting ligands on target cell surface (figure taken from reference 49).

Table 1.2. Surface receptors of human NK cells and their respective interacting ligands on target cell (data taken from reference 46 and 47).

Receptor	Ligand	Function
KIR2DL1 (CD158a)	HLA-C2	Inhibitory
KIR2DL2/3 (CD158b)	HLA-C1	Inhibitory
KIR3DL1	HLA- Bw4	Inhibitory
KIR3DL2	HLA-A11/A3	Inhibitory
NKG2A(CD94/CD159a)	HLA-E	Inhibitory
KIR2DS1	HLA-C2	Activating
FcγRIII (CD16)	IgG	Activating
NKG2C(CD94/CD159c)	HLA-E	Activating
CD2	LFA-3 (CD58)	Co-activating
NKG2D (CD314)	ULBPs, MICA, MICB	Co-activating
NKp30 (CD337)	B7-H6	Co-activating
NKp44 (CD336)		Co-activating
NKp46 (CD335)		Co-activating
2B4 (CD244)	CD48	Co-activating
DNAM-1 (CD226)	PVR (CD155), Nectin-2 (CD112)	Co-activating, adhesion
LFA-1 (CD11a/CD18)	ICAM-1 (CD54)	Co-activating, adhesion, granule polarization

*Co-activating receptors are classified as receptors that do not induce strong activating signal by themselves and only activate NK cell in the presence of other co-activating receptors[46].

In addition to regulation by the different surface receptors, activity of the NK cells is also regulated by various cytokines. Recent data showed that NK cells require priming by distinct cytokines in order to achieve full effector potential, highlighting the intricate interactions between NK cells and other components of the immune system. For instance, NK cells are known to respond to interleukin 2 (IL-2), IL-12, IL-15 and IFNs (α, β and γ), which enhance NK cell's proliferation as well as cytolytic, secretory and anticancer functions[59,61].

Upon viral infection, NK cells are recruited to the site of infection by chemokines, while transformed cells, such as cancer, likely first encounter and interact with peripheral blood and tissue-resident NK cell in their neighborhood[48–50]. When NK cell gets in contact with an abnormal target, a series of well controlled molecular events occur in sequence, including NK cell adhesion, receptor-ligand conjugation and signaling, lytic granule polarization and degranulation or activation of other cytotoxic mode, and cytokine production (e.g., IFN-γ) by NK cells[48,49,51,52]. However, it is not yet clear which receptor-ligand interactions provide the initial signals for target recognition and engagement, and which account for turning on a particular cytotoxic mechanism of NK cell (refer to discussions below).

1.3 Major cytotoxic mechanisms of NK cell

NK cell can elicit direct target cell killing through multiple cytotoxic mechanisms, including lytic granule-mediate apoptosis, death ligand-mediated apoptosis, and necrosis (Fig. 1.2)[1,2,31,51,53–55]. The lytic granule-mediated cytotoxicity is considered the principal pathway by which NK cells kill and eliminate abnormal cells[2,56]. Upon formation of

proper cytolytic conjugation with target cell, lytic granules that contain perforin and granzymes (a type of protease) are polarized and translocate from NK cell into the target cell in an oriented manner through membrane pores formed by perforin. Granzymes are subsequently released inside the target and induce target cell death through proteolysis and intrinsic apoptosis[1,2,51,56,57]. The second major cytotoxic mechanism of NK cells is mediated by death receptor-ligand interaction. NK cells are known to express a variety of death ligands, such as Fas ligand (FasL), tumor necrosis factor (TNF) and TNF-related apoptosis inducing ligand (TRAIL). Through ligation of these death ligands with their respective cognate death receptors expressed on the target cell surface, target cell death is activated by death receptor-mediated extrinsic apoptosis[2,51,58]. Compared to the above two signaling pathways to apoptosis, target cell death by NK cell-induced necrosis is only reported in a few studies and it is unclear whether such cytotoxic mode is relevant at the physiological level or only occurs in *in vitro* NK cell killing assays[54,55].

In addition to triggering direct cytotoxicity, another major function of NK cell is to activate other immune cell types by secreting effector cytokines and chemokines that influence the host's immune response[1,2,31,51,59]. Interferon gamma (IFN-γ) is considered a particularly important NK cell-secreted cytokine and NK cell is the major cell type that secrets IFN-γ upon inflammatory response[51,60–62]. For instance, IFN-γ produced by NK cell can trigger antigen-presenting cells (APCs) to up-regulate expression of MHCI molecules and activate macrophage to kill intracellular pathogens[63,64]. IFN-γ from NK cell also contributes to activate T helper cells and the subsequent adaptive immune response[1,2,51,53,62]. It is well established that NK cell exerts control over parasitic infections, mostly through IFN-γ production[59].

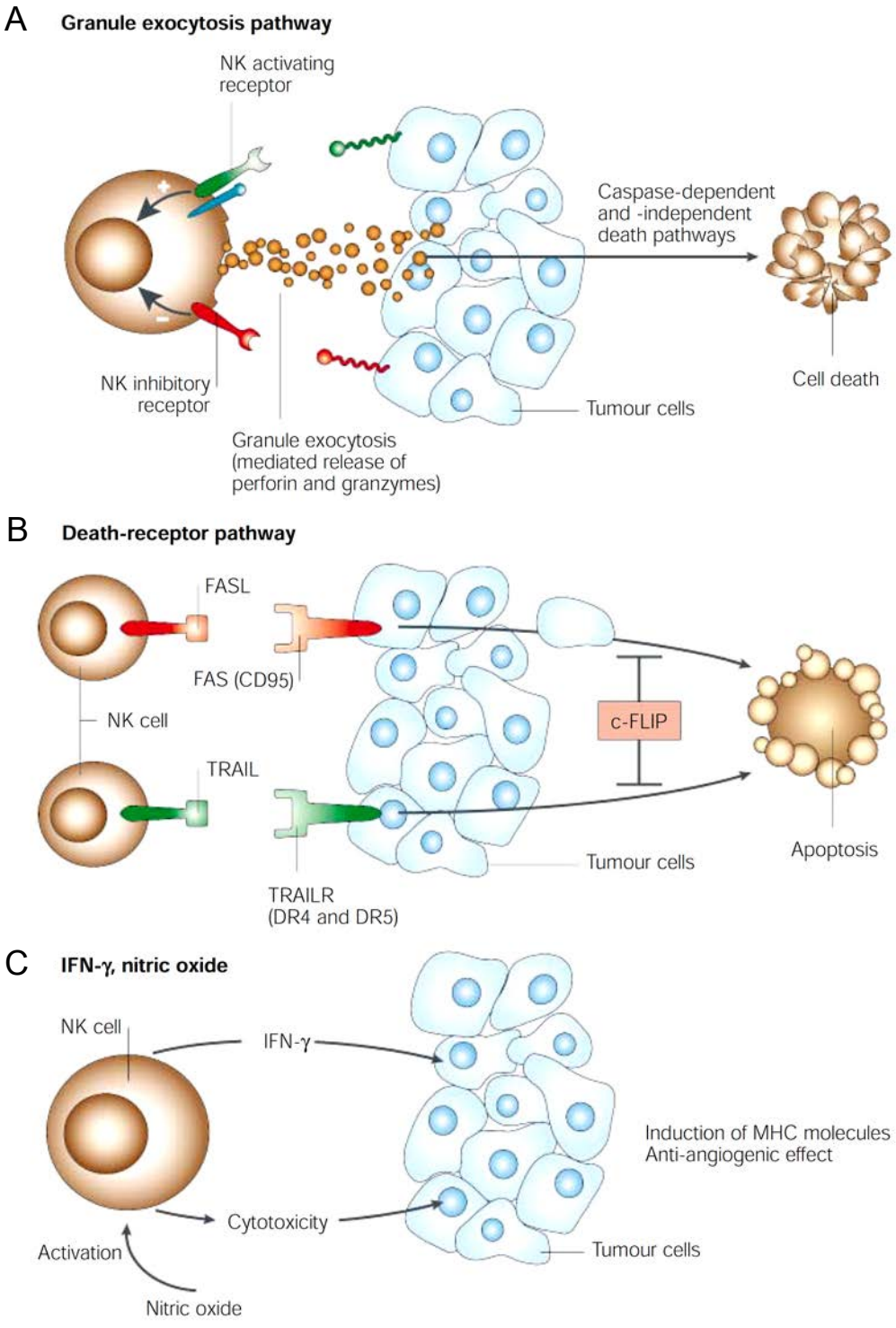

Figure 1.2 Major cytotoxic mechanisms and functions of NK cell (figure taken from reference 51).

1.4 NK cell activity against virus-infected and cancer targets

As mentioned in section 1.2, NK cells can recognize and kill abnormal cells that express few or no MHC-I proteins on the cell surface. MHC-I molecules are recognized by various inhibitory receptors on NK cell surface, which upon binding to their respective ligands on target cell surface, block the cytotoxic activity of NK cells[43]. As MHC-I molecules are constitutively expressed on all nucleated cells and often down-regulated as a result of viral infection or cellular transformation, this missing-self recognition mechanism allows NK cells to selectively eliminate infected and transformed cells and to spare normal, healthy cells[43–45]. Therefore, virus-infected cells and cancer cells are the two major targets for NK cells. NK cell response and function have been evaluated with respect to a wide range of viral infections, including the arenaviruses, herpesviruses, herpes simplex virus, orthomyxoviruses (influenza virus) and picornaviruses[60,65–73]. NK cells are recruited to the site of infection by chemokines and perform their cytotoxic function mainly through perforin-dependent cytotoxicity, IFN-γ secretion and sometimes death ligands induced programmed death[48]. NK cells also contribute to the control of parasitic infections, mostly through IFN-γ production[48]. Although NK cells have been found to respond to infections triggered by other classes of pathogens, the best evidence for their importance in immune defense is with viruses[60].

The most well-known mechanism underlying the antitumor activity of NK cells is through upregulation of ligands for NK cell activation receptors and/or loss of MHC-I molecules on tumor cells[48]. While cytotoxic NK cells directly eliminate tumor cells, regulatory NK cells are believed to also play an important role in the antitumor activity by orchestrating the complex interaction of other immune cell types through secreted

cytokines and chemokines[24,74,75]. Increasing evidence demonstrates that a wide variety of immune cell types are constituents of the tumor and tumor microenvironment, playing critical roles in modulating oncogenesis, metastasis and tumor response to chemotherapy[1,26,51,74,76,77]. The immunogenicity of tumor is believed to originate from tumor-specific antigen peptides, generated by mutation or viral infection[26,78]. These antigens are either presented on the cancer cell surface, e.g., by major histocompatibility (MHC) molecules, or released, subsequently activating anticancer T cell or NK cell response directly or through macrophages and dendritic cells (DCs). An emerging hallmark of malignant cancer is its capability to evade the above immune detection and elimination[1,51,76]. For instance, diverse tumor types were found to downregulate MHCI molecules, which attenuates their recognition by $CD8^+$ T cell, significantly damping the antitumor T cell response[79,80]. In contrast to T cells, lower expression of MHCI molecules enhances target recognition by NK cell and the subsequent NK cell-mediated cytotoxicity, due to reduced inhibitory signaling through the inhibitory receptors, KIRs[44,46,51,79,81]. Moreover, cancer cells often upregulate surface expression of ligands, such as the NKG2D ligands (MICA, MICB and ULBPs), which are binding partners of the activating receptors of NK cell[52,82–86]. The above features render cancer cells more sensitive to NK cell killing, making NK cell potentially a better therapeutic candidate for adoptive cell transfer to treat cancer[51,76].

Most previous studies examined the dynamic control of NK-cancer cell interaction and its mechanistic basis using ensemble killing assays[86–90]. Although informative, such ensemble-averaged results are intrinsically deficient, especially at the quantitative level, as NK-cancer cell interaction naturally occurs at the individual cell level. Single cell

studies of NK-cancer cell interaction are comparatively limited, yet they already provided intriguing new kinetic data that were missed by traditional bulk assays[54,91–93]. For instance, by utilizing microchip-based time-lapse imaging, a number of research groups quantified individual NK-cancer cell interactions and uncovered several interesting characteristics of NK cell activity, including: (1) NK cells operate independently when lysing a single cancer cell[92]; (2) lysis is most probable during an NK cell's first encounter with a target[92]; (3) approximately half of the NK cells do not kill any cancer targets at all, whereas a small population of NK cells were responsible for the majority of cancer cell killing[54]; and (4) secretion of interferon-γ (IFN-γ) occurs most often from NK cells that become the least motile upon conjugation with a cancer target, and is largely independent of cytolysis[92]. These findings demonstrate the unique advantage of using single cell analysis to investigate the rate-limiting kinetics and cell-to-cell variability underlying the NK-cancer cell interaction process. However, crucial questions remain unresolved, e.g., whether activity of primary NK cells and cultured NK cell line differs, how NK cell differentially activates different cytotoxic pathways, and how NK cell activity varies against normal and cancer targets as well as distinct cancer types. I therefore aim to investigate these unresolved questions in my PhD study by employing quantitative single cell imaging.

1.5 Cancer immunotherapy

Immunotherapy is broadly classified as a medical treatment of disease by inducing, enhancing, or suppressing the immune response[2,94,95]. In recent years, immunotherapy has attract great interest from both basic scientists and clinicians, particularly given its promising potential to treat cancer. Cancer immunotherapy exerts therapeutic effect by

modulating the body's own immune system to help fight cancer, which are mainly achieved in two ways: either via stimulating the patients' immune system to work harder or smarter to attack cancer cells or providing the immune system with in vitro stimulating components, such as synthetic immune system proteins[96].

The first cancer immunotherapy in fact was developed in the 1890s by William B. Coley, who is known as the "Father of Immunotherapy". This first generation cancer immunotherapy used a mixed bacterial vaccine of heat-inactivated Streptococcus pyogenes and Serratia marcescens, famously known as the "Coley Toxin", to treat cancer patients[97–99]. Nowadays, immunotherapy is a very active area of cancer research. Many basic scientists and clinicians are exploring new technologies and strategies for cancer immunotherapy. In 2018, four reviews on cancer immunotherapy were published in the same issue of SCIENCE (Vol 359, Issue 6382)[100–103]. It is obvious that cancer immunotherapy plays a more and more important role in the development of more effective anticancer therapy. The above four reviews describe opportunities and challenges for cancer immunotherapy from four treatment approaches, that is, personalized vaccines[102], chimeric antigen receptor (CAR)-T cell[101], microbiome in cancer immunotherapy[100]and immune checkpoint blockade[103]. In these reviews, the scientists analyzed the mechanism, therapeutic effects and applications as well as the commercialization prospects of these treatment approaches. They also pointed out that a more personalized approach will become more important and that new immunotherapies and immunotherapy-based combination approaches will likely become the main treatment modality for cancer treatment in the near future.

There are currently two major types of cancer immunotherapy, which are

summarized and classified in figure1.3. One works through the activation of immune cells, including cancer vaccines, agonists of the immune system, immune checkpoint inhibitors and cellular therapy. The second type works by targeting and inactivating the tumor, using bacterial toxins, oncolytic viruses and monoclonal antibodies. Since bacterial toxins and oncolytic viruses are highly toxic and with activity that may not be easily controllable, now monoclonal antibodies are more commonly used to target tumors. Monoclonal antibodies mostly involve synthetic versions of immune system proteins, which are designed to attack a specific part of the tumor cell.

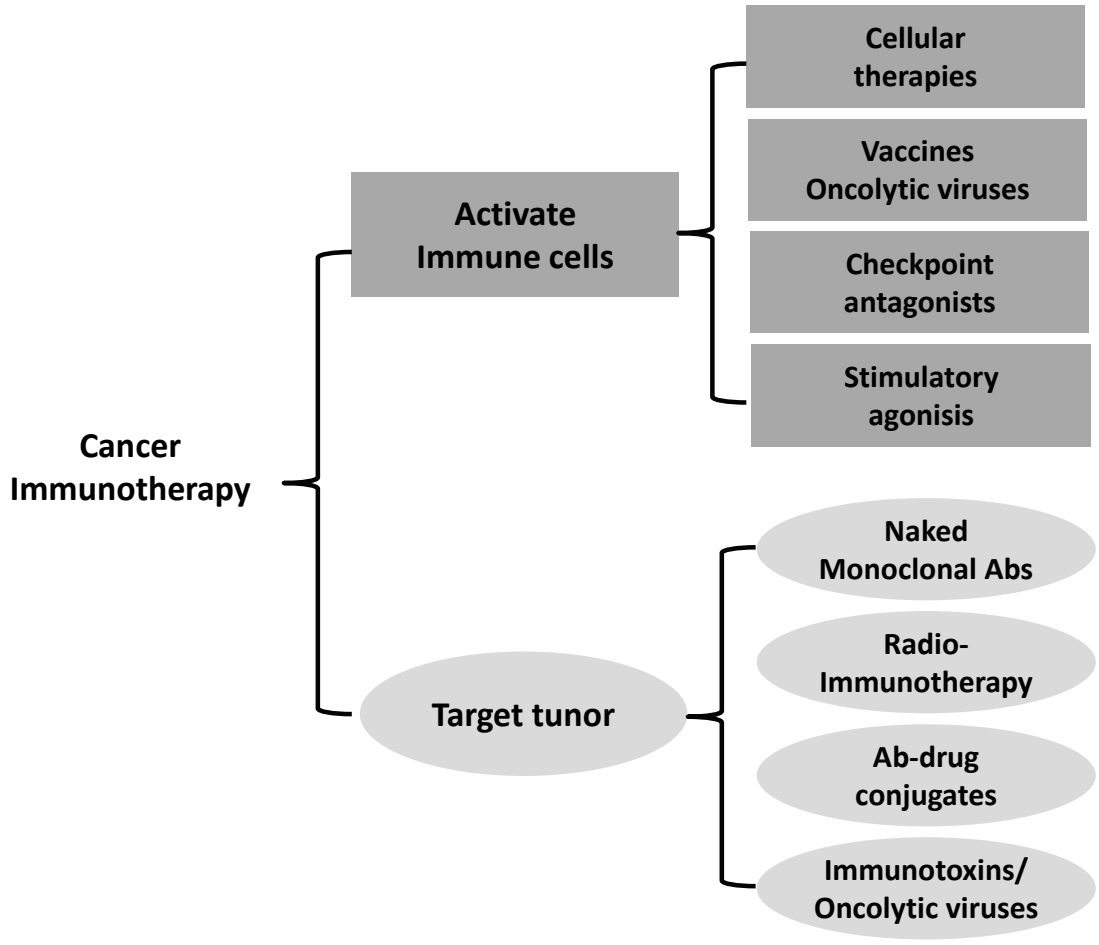

Figure 1.3. Summary and classification of current approaches to cancer immunotherapy.

Among the new generation of cancer immunotherapies, the CAR-T cell therapy is seen as the front runner in cellular therapies, while the CTLA-4 and PD-1 Checkpoint antagonists are the most advanced in research and also clinical application. The NK cell immunotherapy has also obtained significant breakthrough in recent years. Although research on NK cell immunotherapy started comparatively late, the therapeutic development of CAR-engineered NK cells for treating various malignant tumors has made significant progress. It was reported that human NK cell line, NK-92, and primary NK cells that were engineered to express an EGFR-specific CAR targeting both wtEGFR and EGFRvIII showed the feasibility and efficacy of EGFR-CAR-armed NK cell activity against glioblastoma[104]. Meanwhile, more and more studies focusing on elucidating the immune checkpoint molecules affecting NK cell activity are also carried out[105]. The review by Beldi-Ferchiou Asma et al. nicely summarized the different immune checkpoint molecules expressed on NK cell surface and their respective functions (refer to Table1.3 taken from the review, reference 105)[105]. Results from my PhD study on the target dependence of NK cell cytotoxic activity on inhibitory and activating NK cell receptors also provided new insight for understanding the immune checkpoint molecules of NK cells towards distinct cancer targets.

Table 1.3. Overview of immune checkpoint molecules expressed on NK cells: pattern of expression, ligands, and impact on NK cell functions (table taken from reference 105).

Inhibitory Immune	Inhibitory Immune	Inhibitory Immune	Inhibitory Immune
PD-1	Activated T and B cells, NK cells, natural killer T (NKT) cells, ILC-2 cells and myeloid cells.	PD-L1 (B7-H1) and PD-L2 (B7-DC)	Inhibition of NK cell cytolytic activity and cytokine production.
CTLA-4	Treg cells, Activated T and B cells, Activated mouse NK cells, Human NK cells?	B7-1 and B7-2	Inhibition of mouse NK-cell IFN-γ production. Direct effect on human NK cells not documented.
TIM-3	NK, T, NKT and myeloid cells.	Galectin-9 HMGB1 CEACAM1	Dual role (inhibition/activation of NK cell functions) depending on the experimental or linical setting.
T Cell Immunoglobulin and ITIM Domain (TIGIT)	NK cells, T cells.	CD112 (PVRL2) CD155 (PVR)	Inhibition of NK cell functions.
LAG-3	Activated T and NK cells, Treg, B cells, plasmacytoid dendritic cell (DC), NKT	MHC class II molecules	The impact of LAG-3 on NK cell functions is controversial and not well documented
Inhibitory KIRs	NK cells, CD8 T cells.	MHC class I molecules	Inhibition of NK cell functions.
NKG2A	NK cells, CD8 T cells.	HLA-E (non-classical MHC class I molecule)	Inhibition of NK cell functions.

1.6 Objective of the study

The overall objective of my PhD study is to investigate the rate-limiting kinetics and heterogeneity in NK-cancer cell interaction, and elucidate the underlying molecular and cellular mechanisms. By monitoring NK-target cell interaction at the single cell level using several live-cell fluorescent reporters and time-lapse imaging, I first measured kinetics of primary NK cells and cultured NK cell line, NK92-MI, against a model cancer cell line, U-2 OS, which revealed differential killing dynamics mediated by distinct cytotoxic pathways. I then further examined how cytotoxic dynamics of primary NK cells were differentially activated against one normal and four cancer cell lines that showed variable sensitivity to NK cell killing. By perturbing NK-target cell interaction using neutralizing antibodies to block activity of specific NK cell receptors and correlating the data with flow cytometry analysis of surface ligand expression on the target cells, I pinpointed key regulatory components of the NK cell machinery that control NK cell cytotoxic activity. Overall, my PhD study not only provided novel and original results that elucidated the dynamic control of NK-target cell interaction through collective signaling from multiple signaling pathways and molecular interactions but also revealed new mechanistic insight that may guide development of NK cell therapy in the clinical context.

Chapter 2 Research Methodology

2.1 Isolation of primary NK cells from human blood

Primary human NK cells were isolated from fresh human buffy coat (within 24 hours of blood donation) obtained from the Hong Kong Red Cross. Briefly, human buffy coat was diluted in plain RPMI1640 medium (Gibco, Thermo Fisher) and gently added onto the top of Ficoll-Paque Plus solution (GE Healthcare), followed by low speed centrifugation. After the centrifugation, four layers appeared as a result of the density gradient and differential migration. The upper layer is plasma. The interface between the plasma and the Ficoll-Paque Plus solution is the layer of Peripheral Blood Mononuclear Cells (PBMCs), which mainly consist of lymphocytes, monocytes and a small amount of platelets. The bottom layer below the Ficoll-Paque Plus solution is erythrocytes and granulocyte. NK cell population was further purified from the PBMCs by negative selection using the EasySep Human NK Cell Enrichment Kit (STEMCELL Technologies), according to manufacturer's protocol. Based on my experience of primary NK cell isolation from human blood samples, in the summer months (mostly from late June to early September) the quality of isolated primary human NK cells was not as stable and consistent as those obtained in the rest of the year. The large variation in primary NK cells size, the often extremely high (>12%) or low (<3%) primary NK cells yield and also low percentage of CD56+ population of the isolated cells were strong evidences that indicated the poor quality of the NK cell prep in the summer months. The storage condition of the fresh human buffy coat and variation of the blood donors'

healthy condition might the two most possible factors that led to poor prep quality. For all experiments, I only used NK cell prep with purity higher than 90% (measured by FACS analysis of CD56 staining). Isolated human NK cells were either used immediately for experiments or cultured for 3 days at a density of $1x10^6$ cells/ml in RPMI 1640 medium (Gibco, Thermo Fisher) containing 10 ng/ml recombinant human IL-2 (Gibco, Thermo Fisher), 10% heat-inactivated Fetal Calf Serum (FCS, Gibco, Thermo Fisher), 100 U/ml penicillin and 100 μg/ml streptomycin (Gibco, Thermo Fisher), prior to usage.

2.2 Cell line and cell culture

The cultured NK cell line, NK-92MI (CRL-2408, ATCC), was maintained in MyeloCult H5100 Medium (STEMCELL Technologies). Isolated primary human NK cells were maintained in RPMI 1640 medium (Gibco, Thermo Fisher) containing 10 ng/ml recombinant human IL-2 (Gibco, Thermo Fisher), 10% heat-inactivated Fetal Calf Serum (FCS, Gibco, Thermo Fisher), 100 U/ml penicillin and 100 μg/ml streptomycin (Gibco, Thermo Fisher). The normal and cancer cell lines were cultured in appropriate medium supplemented with 10% Fetal Calf Serum (FCS, Gibco, Thermo Fisher), 100 U/ml penicillin and 100 μg/ml streptomycin (Gibco, Thermo Fisher). Specifically, U-2 OS was maintained in McCoy's 5A (Modified) Medium; MCF7 was maintained in RPMI 1640 Medium; SMMC-7721, HeLa and LO2 were maintained in Dulbecco’s modified Eagles Medium (DMEM).

2.3 Generation of fluorescent reporter cell lines and isogenic clones

The retroviral Förster Resonance Energy Transfer (FRET) construct that reports on granzyme-B proteolytic activity is a generous gift from Dr. Paul Choi (Genome Institute of Singapore) and consists of a cyan (CFP) and a yellow (YFP) fluorescent protein linked by a peptide substrate, VGPDFGR, specific to granzyme-B[91]. The FRET construct that reports on caspase-8 activity is a generous gift from Dr. Peter Sorger (Department of Systems Biology, Harvard Medical School) and consists of CFP and YFP fused by a peptide linker, GLRSGGIETDGGIETDGGSGST, which is a substrate specific to caspase-8[58]. LO2, SMMC-7721, U-2 OS, HeLa and MCF7 cells were infected with the retroviral granzyme-B FRET construct and/or transfected with the regular caspase-8 FRET plasmid. Moreover, I further infected the reporter cells with a retroviral construct, IMS-RP, which encodes a monomeric red fluorescent protein targeted to the inter-membrane space of mitochondria by fusion to the leader peptide of SMAC (a generous gift from Dr. Peter Sorger, Harvard Medical School[58]). By monitoring the abrupt transition from punctate to smooth localization of IMS-RP fluorescence, mitochondrial outer membrane permeabilization (MOMP), i.e., the committed step leading to the onset of apoptosis, can be scored relative to FRET signal change by live-cell imaging. Then, isogenic clones were selected to generate stable FRET reporter and IMS-RP reporter cell lines. All the isogenic clones had been profiled in co-culture with both the NK cell line, NK-92MI, and primary NK cells to examine their sensitivity to NK cell killing. The isogenic clones which exhibited the sensitivity to primary NK cell killing that was most similar to their respective parental lines were selected as the model fluorescence reporter clones for performing the live-cell imaging assays.

2.4 Chemicals, siRNA oligo and neutralizing antibodies

Ethylene glycol tetraacetic acid (EGTA, Sigma-Aldrich) was used at 0.8 mM to chelate calcium in the culture medium and block the calcium flux inside the cells. Concanamycin A (CMA, Santa Cruz Biotechnology) was used at 1 μM as a saturating dosage and titrated down to 10, 5, 4, and 2 nM to inhibit perforin activity. LysoBrite (AAT Bioquest) was used to stain the lytic granule for live-cell tracking, according to manufacturer's protocol.

SiRNA oligo to silence caspase-8 (5'-UGGAUUUGCUGAUUACCUAuu-3') was custom synthesized by Dharmacon and used at a final concentration of 40 nM. On-Target plus siControl (D-001810-01, Dharmacon) was used as non-targeting siRNA control. All siRNA transfections were performed using HiPerFect (Qiagen). Experiments were conducted after 48 hours of gene silencing.

To block the activity of various NK cell receptors and ligands, the following neutralizing antibodies were used. The anti-Fas neutralizing antibody (human, Clone ZB4, EMD Millipore) was used at 1.5 μg/ml. Purified anti-human HLA-A,B,C antibody (Clone W6/32, Biolegend) was used at 5 μg/ml. CD94 (Clone DX22, Biolegend), NKG2D (Clone 1D11, Biolegend), NKp46 (Clone 9E2, Biolegend), DNAM-1 (Clone 11A8, Biolegend) were used at 10 μg/ml.

2.5 Time-lapse microscopy and image analysis

Cells were plated in 24-well glass-bottom imaging plate (MatTek) or 96-well μ-plate (ibidi), and cultured in CO_2-independent medium without phenol red (Gibco, Thermo

Fisher) supplemented with 10% heat-inactivated FCS, 4 mM L-glutamine, 100 U/ml penicillin and 100 μg/ml streptomycin. Cells were imaged by a Nikon Eclipse TE-2000 inverted microscope with either a 20X phase contrast objective (NA = 0.75) or a 20X plan Apo objective (NA = 0.95). The microscope was enclosed in a humidified chamber maintained at 37°C. Images were acquired every 2, 4 or 10 minutes, varied between experiments. Images were viewed and analyzed using the MetaMorph software (Molecular Devices). Target cell death was scored morphologically by blebbing followed by cell lysis. The onset of apoptosis is scored by an abrupt transition from punctate to smooth localization of the mitochondria reporter, IMS-RP. The specific cytotoxic mode that led to target cell death was scored based on granzyme-B or caspase-8 specific FRET signal. To quantify the time courses of FRET signal, an automatic cell tracking program based on Matlab, which was developed by Dr. Bo Huang (Senior Research Assistant of our research group), was used. The program consists of image analysis procedures that sequentially segment the individual cells, track them in time, as well as measure and ratio the cellular CFP and YFP fluorescence intensity.

2.6 Flow cytometry

Cancer cells were collected, washed once and then re-suspended in cell staining buffer (Biolegend). $1x10^6$ cells were then stained with different dye-conjugated primary antibodies at 1 μg/ml or 5 μg/ml in 100 μl cell staining buffer for 30 minutes at 4°C. The stained cells were washed once in the staining buffer and once in PBS, then stained with Zombie NIR fixable viability kit (Biolegend) at 1:30 dilution in PBS for 20 minutes at

room temperature. After staining, the cells were washed once and re-suspended in the cell staining buffer. Fluorescence intensities of the surface markers were analyzed by flow cytometry measurement conducted with a FACSCanto II cytometer (BD Biosciences). Primary antibodies and the corresponding control used for this analysis include: FITC Mouse IgG1 κ Isotype Control Antibody (Clone MOPC-21, Biolegend), FITC anti-human HLA-A,B,C (Clone W6/32, Biolegend), FITC anti-human ICAM-1/CD54 Antibody (Clone DX2, Biolegend), FITC anti-human Fas /CD95 Antibody (Clone DX2, Biolegend), APC Mouse IgG1 κ Isotype Control Antibody (Clone MOPC-21, Biolegend), APC anti-human Nectin-2/ CD112 Antibody (Clone TX31, Biolegend), APC anti-human PVR/ CD155 Antibody (Clone SKII.4, Biolegend), PE Mouse IgG2b κ Isotype Control Antibody (Clone MPC-11, Biolegend), Human MICA PE-conjugated Antibody (Clone 159227, R&D Systems), Human MICB PE-conjugated Antibody (Clone 236511, R&D Systems), Human ULBP-2/5/6 PE-conjugated Antibody (Clone 165903, R&D Systems).

Chapter 3 Quantitative characteristics of cytotoxic dynamics of primary human NK cell at the single cell level

3.1 Cytotoxic dynamics of primary human NK cell are distinct from cultured NK cell line, NK92-MI

To quantitatively elucidate the cytotoxic dynamics of primary NK cells against adherent cancer target, I first measured the killing activity of primary NK cell in comparison with a widely studied model NK cell line, NK92-MI, by live-cell imaging. NK-92MI cell line was generated by Tam YK, et al., by transfecting an MFG-hIL2 vector which contained human IL-2 cDNA to the parental cell line NK-92[106]. As IL-2 is an important cytokine promoting NK cell viability and cytotoxicity, and also that the NK-92MI as well as its parental cell line, NK-92, lack KIRs that inhibit NK cell killing activity via KIRs-MHCI molecule conjugation, NK-92MI is highly activated and exhibits strong cytotoxicity towards a broad range of targets[46,106–108]. In the past decades, numerous studies had been carried out with the NK-92MI cell line, and plenty of NK cell killing mechanisms were characterized using NK-92MI as a human NK cell model. According to results in the literature, the superior killing activity of NK-92MI cells were mainly through perforin and granzyme-B mediated cytolytic pathway. NK-92MI cells also had been considered as a highly promising candidate for aoptive cell transfer immunotherapy[91,106,108–111]. Therefore, in my PhD study I chose NK-92MI as a model

cell line and compare its cytotoxic dynamics and characteristics with those of primary NK cells purified from human blood. U-2 OS, a human epithelial cancer cell line derived from osteosarcoma, was used as the model cancer target. Primary human NK cells were freshly isolated from blood of healthy donor by negative selection, and used either immediately for experiments or after 3-day culture in medium supplemented with moderate level of Interleukin 2 (IL-2, 10 ng/ml). Figure 3.1A shows time-lapse images of primary NK cells or NK92-MI in co-culture with U-2 OS. The small, suspending NK cells are easily distinguishable morphologically from the large, adherent target cancer cell, U-2 OS, based on phase-contrast images. Target U-2 OS cell death was scored by cell rounding and lysis, based on which I plotted the killing kinetics as cumulative survival curves of the target U-2 OS cells (Fig. 3.1B). Three distinct dynamic features were immediately observable that varied between primary NK cells and NK92-MI. Firstly, the size of NK92-MI cells was significantly larger than that of the primary NK cells. The average diameter of NK92-MI cells were about 3-fold larger than the freshly isolated primary NK cells. Secondly, freshly isolated primary NK cells changed from ball-like shape to an elongated, polarized morphology after 6-10 hours in culture, while the majority of NK92-MI cells did not prominently exhibit such elongated morphology. Polarization is known to be important for NK cell activation, migration and target recognition [112]. However, the lack of polarization in NK92-MI did not appear to affect its killing efficiency, indicating that NK92-MI may be highly activated and thus do not require the polarization, e.g., for target recognition. Thirdly, contacts between primary NK and U-2 OS cells (scored by co-localization of the two cell types) were in general short, less than 20 minutes, while NK92-MI often assumed very long contact (> 1 hour)

with the target cells. Fourthly, at the same NK-to-target cell ratio (2:1), NK92-MI killed more than 20-fold faster than fresh primary NK cells. Increasing the concentration of primary NK cells or pre-activating them with IL-2 for 3 days significantly increased the NK cell cytotoxic activity (Fig. 3.1B).

Most literature on NK cell cytotoxicity focused on the rapid target killing by way of lytic granule transfer, which results in target cell death due to granzyme-B mediated proteolysis. The much slower killing dynamics that I observed with primary NK cells in culture led me to investigate whether the lytic granule/granzyme-B pathway played a lesser role in the cytotoxicity of primary NK cells as compared to NK92-MI. To monitor lytic granule/granzyme-B specific NK cell killing, I generated fluorescent U-2 OS reporter cell line that stably expresses a Förster Resonance Energy Transfer (FRET) construct, consisting of a cyan (CFP, donor) and yellow (YFP, receptor) fluorescent protein linked by a peptide substrate specific to granzyme-B, i.e., VGPDFGR [91]. Upon lytic granule transfer and release of granzyme-B into the target cell, granzyme-B cleaves the peptide linker of the FRET reporter and thus energy transfer from CFP to YFP is lost, resulting in decrease of YFP fluorescence (denoted in green) and increase of cyan fluorescence (denoted in blue) (Fig. 3.1C). Analysis of the FRET signal preceding individual cell death showed that about 71% of U-2 OS cell death activated by NK92-MI was preceded by a FRET signal change, indicating the cytotoxic process is mainly mediated by the lytic granule pathway and granzyme-B (Fig. 3.1D). However, only about 13% target U-2 OS cell death triggered by fresh primary NK cells (at 5:1 NK-to-target ratio) was preceded by the granzyme-B specific FRET signal change. Pre-activating primary NK cells with IL-2 for 3 days increased granzyme-B mediated killing to about

32%, but the majority of target cell death remained non-granzyme-B dependent. These results point to important mechanistic difference in how primary NK cells elicits killing of adherent cancer target in comparison to the highly activated NK92-MI.

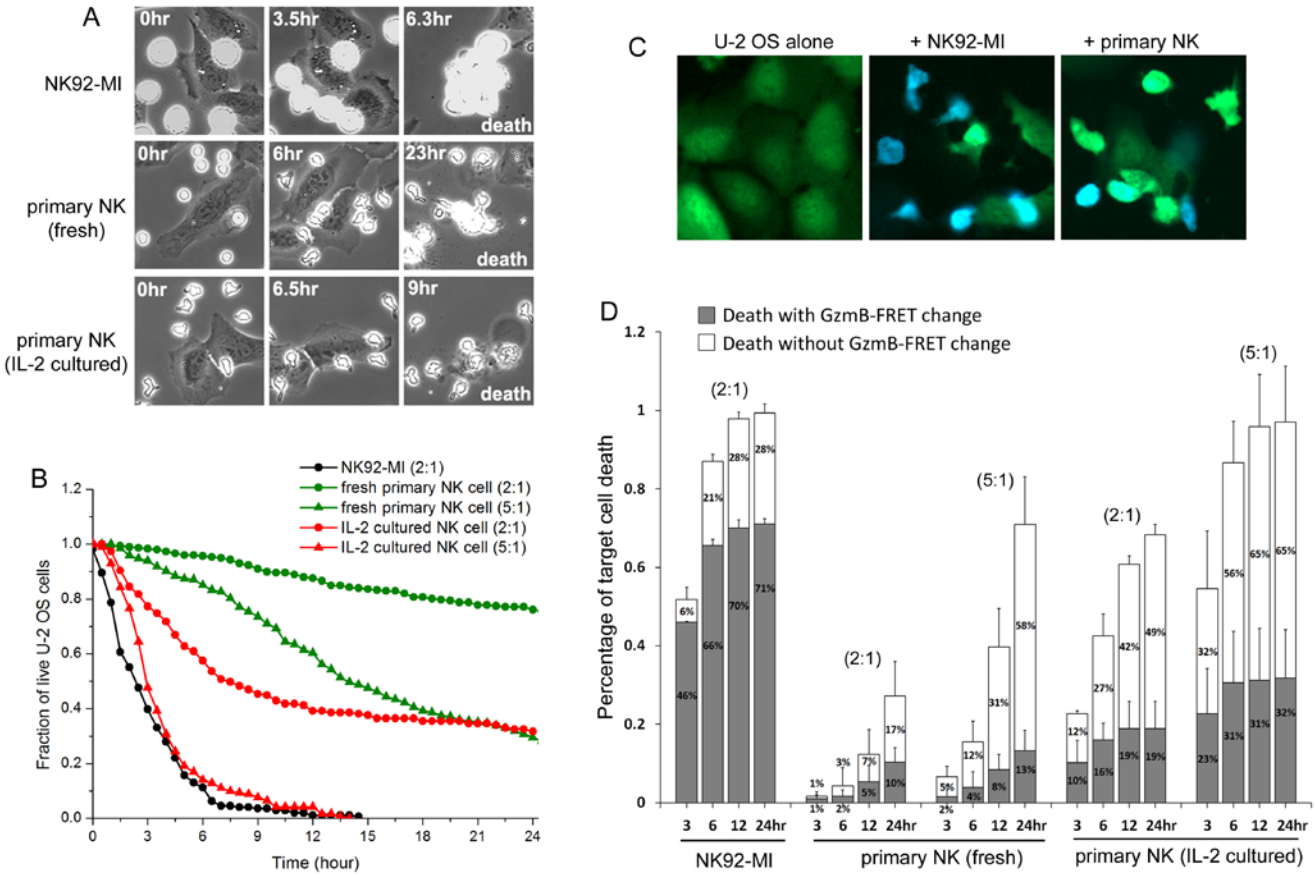

Figure 3.1. Cytotoxic dynamics of primary NK cells are distinct from NK cell line, NK92-MI. (A) Phase-contrast images of distinct NK cells in co-culture with a human cancer cell line, U-2 OS, acquired from live-cell imaging. NK cells were added at time 0 (time is indicated in unit of hours at the upper corner of the still images). Cell death was scored by cell lysis. (B) Cumulative survival curves of target U-2 OS cells at the indicated co-culture condition: with NK92-MI at 2:1 NK-to-target ratio (denoted in black circle); with fresh primary NK cells at 2:1 (green circle) or 5:1 (green triangle) NK-to-target cell ratio; with 3-day IL-2 cultured primary NK cells at 2:1 (red circle) or 5:1 (red triangle) NK-to-target cell ratio. For all imaging experiments with primary NK cells, 50 ng/ml IL-2 was supplemented in the medium. Data were averaged from 2 or 3 independent imaging experiments and the number of cells analyzed ranges from 55 to

115, varied between conditions and experiments. Individual target U-2 OS cells were monitored by phase-contrast and fluorescent time-lapse microscopy, and time from NK cell addition to morphological target cell death was analyzed and plotted as cumulative survival curves. (C) Fluorescent images of the granzyme-B FRET reporter from U-2 OS cells alone (1st column), U-2 OS in co-culture with NK92-MI for 10 hrs (2nd column) and U-2 OS in co-culture with 3-day IL-2 cultured primary NK cells for 10 hrs (3rd column). The images are overlay of the CFP (denoted by blue) and YFP (denoted by green) channels. (D) Distribution of the granzyme-B dependent (solid gray column) and independent (open column) killing of U-2 OS cells by different NK cells at the indicated co-culture conditions. The NK-to-target cell ratio is indicated at the top of the respective data set.

3.2 Granzyme-B independent cytotoxicity of primary NK cell is mainly mediated by Fas ligand

The non-granzyme-B mediated cytotoxicity by primary NK cell could be mediated by two possible mechanisms, one still involving lytic granule but different granzymes (e.g., granzyme M[113]), and the other involving extrinsic apoptosis triggered by death ligand. To examine whether lytic granule transfer is still responsible for target cell death not associated with granzyme-B activity, I used a calcium chelating regent, EGTA, to inhibit lytic granule transfer and measured the consequent NK cell activity. The presence of EGTA significantly attenuated the overall cytotoxicity of primary NK cells and abrogated nearly all target cell death mediated by granzyme-B (Fig. 3.2A), confirming the effect of EGTA in preventing lytic granule transfer and subsequent granzyme release into target cell. After 24 hours of NK-U-2 OS cell co-culture in EGTA, about 40% of U-2 OS cell death that were independent of FRET signal change still occurred (Fig. 3.2A), and the non-FRET associated target cell death increased to about 60% at 36 hours (data not shown). These data suggest that the granzyme-B independent killing by primary NK cells is largely mediated by cytotoxic pathway(s) not involving lytic granule transfer.

Activation of extrinsic apoptosis by death receptor binding is a second well-known, but less studied, mechanism by which NK cells elicit cytotoxicity. To determine whether extrinsic apoptosis is responsible for the granzyme-B independent target cell death that I observed, I knocked down caspase-8, the initiator caspase for extrinsic apoptosis, in U-2 OS cells by RNA interference (RNAi). Knockdown of caspase-8 significantly attenuated primary NK cell cytotoxicity, in particular reducing the percentage of target cell death that is independent of granzyme-B activity (i.e., no change in GzmB-FRET signal) from

about 65% to 25%, strongly suggesting the majority of this population of cell death is activated by caspase-8 mediated extrinsic apoptosis (Fig. 3.2B). As NK cells highly express Fas ligand (FasL)[57], I next investigated whether the observed extrinsic apoptosis was triggered by FasL binding to the death receptor, Fas/CD95, on U-2 OS cell surface. As shown in Figure 3.2C, silencing the FasL signaling pathway by an anti-Fas neutralizing antibody (1.5 μg/ml) particularly attenuated the granzyme-B independent NK cell killing, reducing the extent of U-2 OS cell death with no FRET signal change again from about 65% to 25%, similar to the degree of cytotoxicity attenuation observed with caspase-8 knockdown. Therefore, our results illustrate that FasL is the major death ligand on primary NK cells that contributes to the activation of target cell death through extrinsic apoptosis, although a remaining 25% of granzyme-B independent killing appeared to be mediated by other non-lytic granule cytotoxic mechanism(s), possibly through cytokines, such as TNF-α and Interferon-γ [114,115].

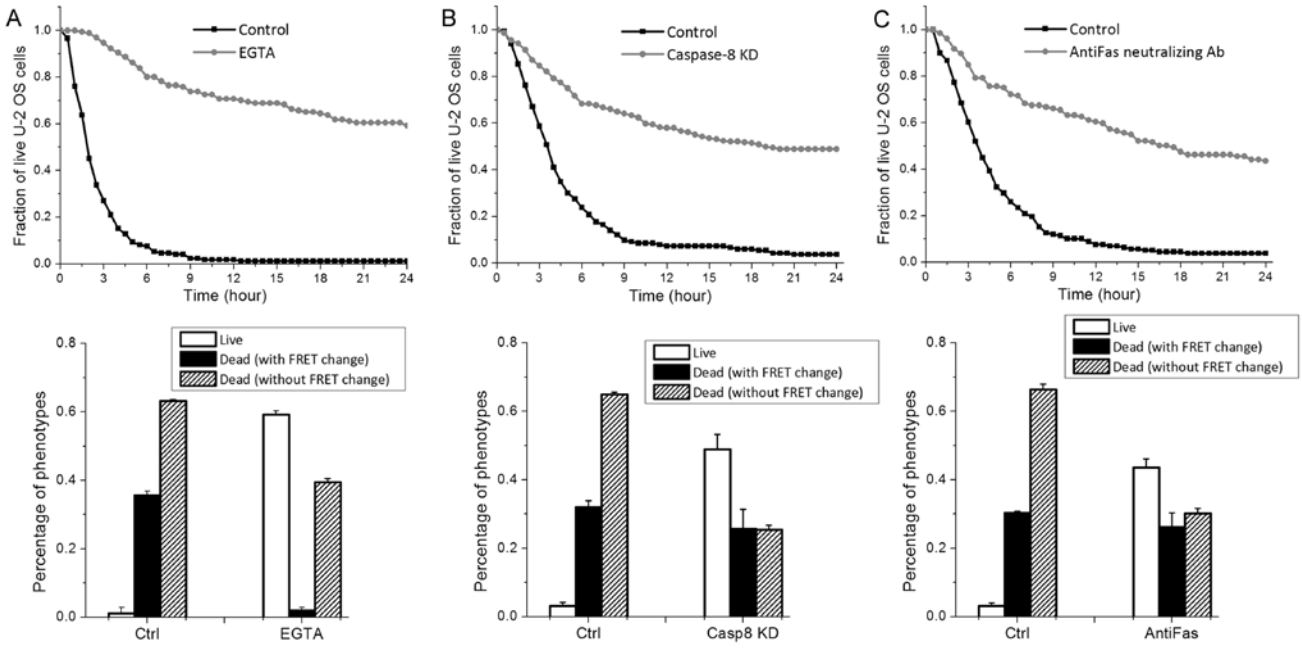

Figure 3.2. Granzyme-B independent killing by primary NK cells is mainly mediated by extrinsic apoptosis induced by FasL. Cumulative survival curves and distributions of granzyme-B and non-granzyme-B dependent target cell death quantified from U-2 OS cells in co-culture with primary NK cells (3-day cultured in IL-2) plus the indicated treatment: (A) 0.8 mM EGTA, (B) RNAi knockdown of caspase-8 and (C) 1.5 μg/ml anti-Fas neutralizing antibody. Data were averaged from 2 independent imaging experiments and the number of cells analyzed ranges from 64 to 155, varied between conditions and experiments.

3.3 Gradual caspase-8 induction triggered by transient FasL binding versus switch-like granzyme-B activation upon lytic granule transfer

The fact that primary NK cells simultaneously activates cancer cell death at least by two distinct cytotoxic pathways, i.e., FasL and lytic granule, raised intriguing questions regarding the rate-limiting kinetics of these two distinct killing modes and how their respective characteristics determine the likelihood of an individual target cancer cell die of one or the other cytotoxic mechanism. As indicated by results shown in Figure 3.1C, target cell killing by the granzyme-B dependent mechanism mostly occurred early, while a significant percentage of the non-granzyme-B dependent target cell death occurred at later time frames. Such kinetic difference between the two distinct killing modes prompted me to further compare their induction characteristics in real time. The FRET signal specific to granzyme-B activation provides a convenient measure to quantify induction dynamics of the lytic granule pathway. In order to also monitor the activation dynamics of extrinsic apoptosis resulting from FasL binding, I engineered another U-2 OS reporter cell line that expresses a FRET construct, consisting of a CFP and a YFP linked by peptide substrate specific to caspase-8[116]. In addition, I incorporated a red fluorescent reporter of mitochondria, IMS-RP[116], in both the caspase-8 and granzyme-B FRET reporter cell lines. As an abrupt transition from punctate to smooth localization of IMS-RP fluorescence corresponds to mitochondrial outer membrane permeabilization (MOMP), the committed step of apoptosis, the IMS-RP reporter allowed me to analyze kinetics of primary NK cell killing (i.e., FRET signal change) relative to the precise onset of target cell death (i.e., MOMP) in real time. And I quantified the FRET signal as ratio of the CFP and YFP fluorescence in individual U-2 OS cell, i.e., an increase in FRET

ratio corresponds to increase of the respective protease activity.

This single-cell analysis revealed distinct activation dynamics of caspase-8 and granzyme-B preceding MOMP. The caspase-8 FRET ratio in individual U-2 OS cell exhibited a gradual increase before MOMP. And the rate of increase accelerated in a step-wise manner for some target cells, indicating caspase-8 in these cells were sequentially activated by FasL-Fas conjugations with multiple primary NK cells (Fig. 3.3A). Moreover, NK-U-2 OS cell conjugations that led to the increase of caspase-8 activity were always short, less than 2 minutes (the frame rate of my imaging experiments). Due to such transient nature of NK-U-2 OS conjugation in activating FasL signaling, very limited amount of caspase-8 was likely activated, thus requiring an extended period of accumulation, and often multiple successful cytotoxic NK-U-2OS conjugations, to reach the threshold of MOMP for triggering target cancer cell death. In contrast, the granzyme-B FRET ratio showed an abrupt, switch-like increase before MOMP and this rapid induction of granzyme-B activity involved a single, sustained NK-U-2 OS cell conjugation that typically persisted for 10-20 minutes (Fig. 3.3B). Hence, primary NK cell killing by lytic granule transfer appeared to occur in an all-or-none manner, and the long NK-target conjugation upon killing by lytic granule transfer was distinct from the transient conjugation for FasL-mediated cytotoxicity, which probably ensures extensive lytic granule transfer and activation of high level of granzyme-B activity to trigger rapid target cell death.

By staining the lytic granule with an acidic organelle marker, Lysobrite, I next studied in more details the dynamics of lytic granule transfer relative to NK-target cell conjugation, the onset of protease activity and target cell death. As shown in Figure 3.3C,

polarized primary NK cell stored the lytic granules in its tail, as it moved and transiently interacted with the target U-2 OS cell. Such localization of lytic granules probably prevents undesirable leakage of lytic granules to target cancer cell in the absence of proper cytolytic conjugation during the constant, transient contact between NK and target cells. Upon recognition and formation of a cytolytic conjugation, the lytic granules translocated to the leading front and then transferred into target cells, with each kinetic step taking about 2 minutes (Fig. 3.3D). The lysobrite imaging results also confirmed there was no lytic granule leakage during all the transient NK-U-2 OS cell interactions. In the presence of EGTA, primary NK cells were still able to recognize and form sustained conjugation with the target U-2 OS cells. However, even though the lytic granules successfully translocated to the NK cell front, further transfer into the target cells was abrogated due to the absence of calcium flux; and the NK cell eventually came off the target after 40 minutes to 1 hour (Fig. 3.3D). As I observed no lytic granule transfer under EGTA treatment, it further indicated that the granzyme-B independent NK cell cytotoxicity is unlikely to be mediated by alternative granzymes. Interestingly, by imaging the caspase-8 FRET reporter together with lysobrite, I found a number of U-2 OS cells exhibited a gradual induction of caspase-8 activation before encountering a sustained lytic NK-U-2 OS cell conjugation followed by lytic granule transfer and rapid target cell death (Fig. 3.3D). This observation revealed that a portion of U-2 OS cells that appeared to die of the lytic granule mechanism were in fact killed by the combined mechanism of FasL and lytic granule; and the FasL pathway contributed to lytic granule-mediated NK cell killing by activating caspase-8 and sensitizing the target cells to MOMP.

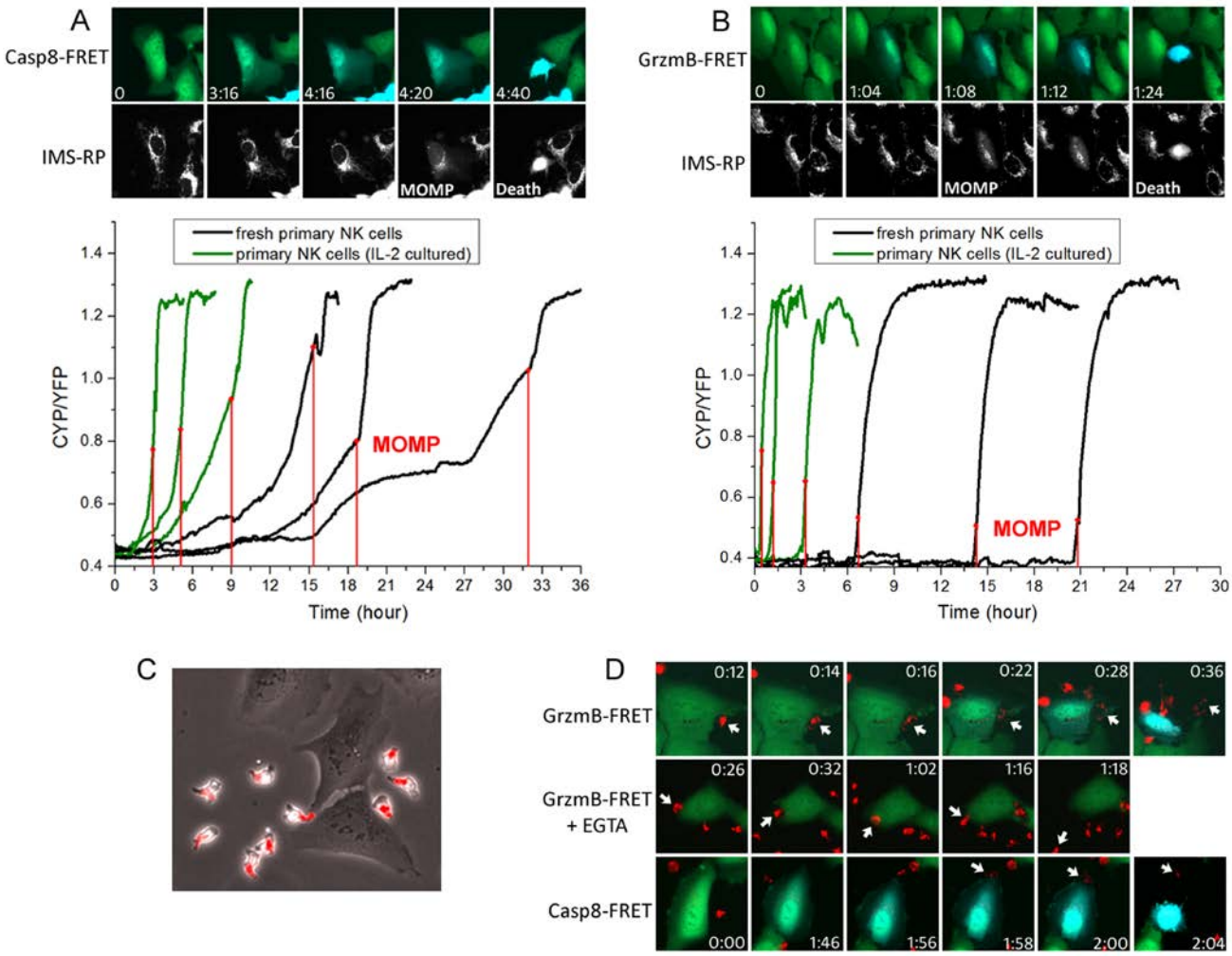

Figure 3.3. The FasL and lytic granule cytotoxic pathways exhibited distinct activation kinetics and involved different types of NK-target cell conjugation. (A) Induction kinetics of caspase-8 by FasL. Upper panel: Still images were obtained from live-cell imaging of caspase-8 FRET reporter. The onset of apoptosis was scored by a change from punctate to smooth distribution in the fluorescence of the mitochondria reporter, IMS-RP (marked as MOMP on the corresponding image). Time is indicated in the unit of hour:minute. Lower panel: Representative time courses of the FRET signal ratio from individual U-2 OS cells, calculated as the ratio of CFP and YFP fluorescence from the caspase-8 FRET reporter. The time of MOMP is indicated by the red vertical line. (B)

Induction kinetics of granzyme-B quantified based on fluorescence of the granzyme-B FRET reporter. (C) Localization of lytic granules in primary NK cells probed by an acidic granule marker, lysobrite. The images were overlay of the phase-contrast and red fluorescent channels. (D) Dynamics of lytic granule upon NK-target cell interaction under the indicated conditions. The images were overlay of the CFP (blue) and YFP (green) fluorescence from the respective FRET reporter and red fluorescence from lysobrite. The specific interacting NK cells are indicated by the white arrows.

3.4 Interleukin 2 promotes cancer target detection by NK cell and increases NK-target cell interaction

In all the experiments discussed above, I supplemented the primary NK-U-2OS cell co-culture with high Interleukin 2 (IL-2, 50 ng/ml), as IL-2 is a well-known cytokine that promotes NK cell survival and cytotoxicity. Previous studies have shown the agonist effect of IL-2 on NK cell cytotoxicity is partly through activating expression of perforin, granzyme-B and FasL[58,117]. Using the single cell imaging assay, I next examined whether IL-2, in addition to transcriptional activation of cytotoxic genes, modulates other aspects of the dynamic control of NK-cancer cell interaction. I first compared the killing kinetics of primary NK cell (3-day cultured) under high (i.e., 50 ng/ml) versus low (i.e., 0.2 ng/ml) IL-2 supplement. Treatment condition of low IL-2, instead of no IL-2, was chosen for the comparison because I found primary NK cell did not survive in culture in the absence of IL-2. High level of IL-2 induced more rapid and extensive U-2 OS cell killing (Fig. 3.4A), and granzyme-B independent killing became an even more dominant cytotoxic mechanism under low IL-2 (Fig. 3.4A). Given that the primary NK cells had been pre-activated by IL-2 for 3 days prior to experiments, the expression level of cytotoxic genes should be relatively similar. Therefore, the dose-dependent effect of IL-2 on NK cell cytotoxicity that I observed was likely due to additional regulatory mechanism(s).

One distinctive dynamic feature that I observed under low IL-2 is that primary NK cells generally assumed less contacts with the target cancer cells, as compared to that under high IL-2. Figure 3.4B shows representative NK cell trajectories near the target U-2 OS cell under high and low IL-2. NK cells under high IL-2 evidently stayed longer to the proximity of U-2 OS cells and were more likely to direct their movement towards the

cancer target, indicating IL-2 promotes target detection by NK cells, possibly by enhancing NK cell sensing of the chemokine gradient secreted by the target cells. The average number of NK-U-2 OS cell contacts per hour (scored by co-localization) is plotted in Figure 3.4C. On average, 13 contacts per hour were observed between NK cells and a target U-2 OS cell under high IL-2, in comparison to 5 contacts per hour under low IL-2. In addition, while contact frequency significantly decreased in time under low IL-2, high IL-2 maintained a relatively constant NK-target cell contact frequency. I observed no significant difference in contact duration under high and low IL-2, with most NK-target cell interactions being of transient nature, persisting less than 4 minutes (Fig. 3.4D). In summary, my results suggest that in addition to transcriptionally activating cytotoxic genes, IL-2 also enhances NK cell cytotoxicity by promoting target detection by NK cells and increasing NK-target cell interaction frequency.

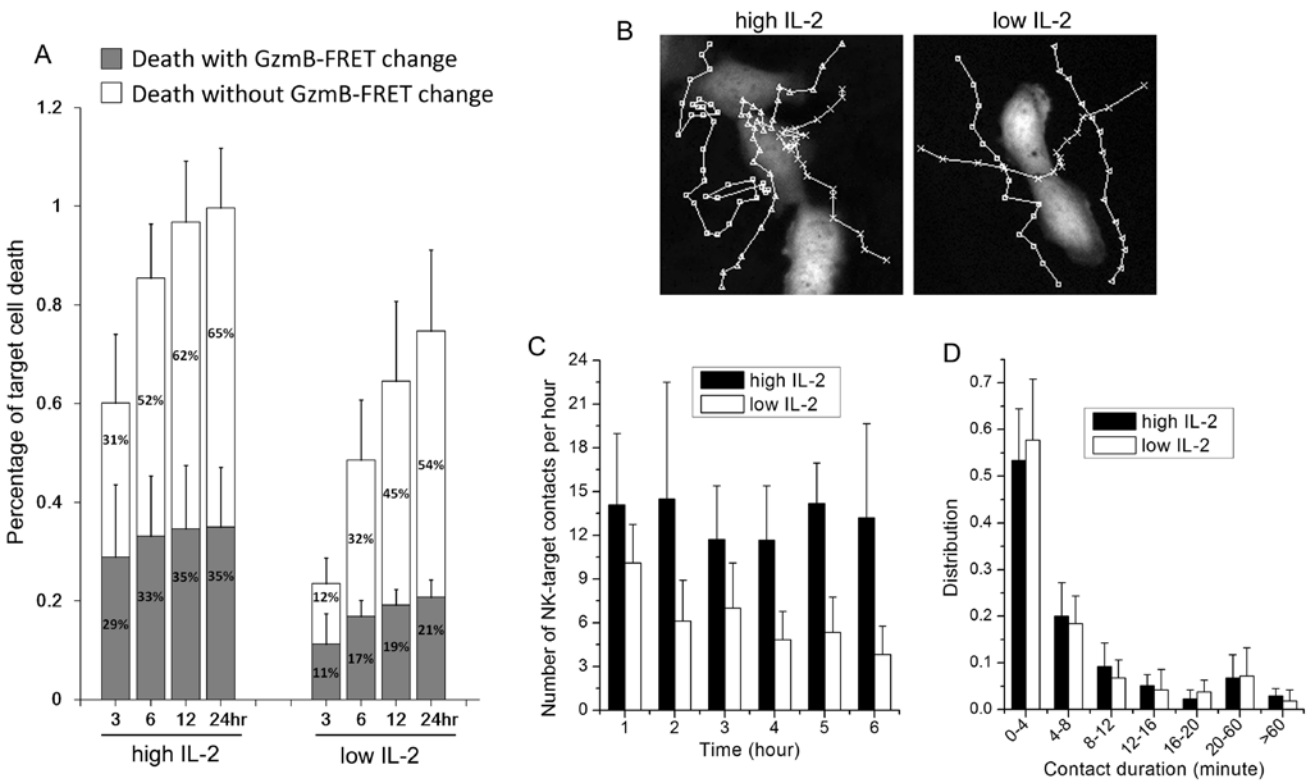

Figure 3.4. IL-2 regulates the directionality of NK cell movement towards the target cell and the frequency of NK-target cell contact. (A) Comparison of primary NK cell (3-day cultured in IL-2) cytotoxicity under high (50 ng/ml) and low (0.2 ng/ml) IL-2 supplement. Data were averaged from 4 independent experiments and the number of cells analyzed ranges from 51 to 84, varied between conditions and experiments. (B) Representative NK cell trajectories, as they move around the target cells under high vs. low IL-2. (C) Average number of contacts per hour and (D) average contact duration between a target U-2 OS cell and NK cells under high vs. low IL-2. Data for each condition were averaged from 10 individual target U-2 OS cells from 2 independent experiments.

Chapter 4 Target specificity of cytotoxic dynamics of primary human NK cell

4.1 Cytotoxic mode and kinetics of primary NK cell depended on target cell type

Based on the live-cell imaging assays elaborated in Chapter 3, I went on to examine how cytotoxic dynamics of primary human NK cell may vary when encountering different target cell types. For this investigation, I chose one normal and four cancer culture cell lines as NK cell targets for comparison, including LO2 (normal hepatic cell line derived by immortalization), HeLa (derived from cervix adenocarcinoma), SMMC-7721 (derived from hepatocarcinoma), MCF7 (derived from breast adenocarcinoma), and U-2 OS (derived from bone osteosarcoma). These cell lines were chosen, as they exhibited variable sensitivity to primary NK cell killing (Fig. 4.1A). Similar to U-2 OS cells, I first generated fluorescent reporter cell lines for each of the four additional cell lines with the granzyme-B FRET (GzmB-FRET) reporter and the mitochondria reporter, IMS-RP, and then selected isogenic clones that exhibited sensitivity to primary NK cell killing similar to the parental lines. As shown in Figure 4.1A, when in co-culture with primary NK cell that were pre-activated by IL-2 for three days and under a NK-to-target cell ratio of 3:1 (this condition was used for all NK-target cell co-culture measurements elaborated in this chapter), the normal cell line, LO2, was the most resistant to NK cell killing, which is consistent with NK cell's function in eliminating abnormal cells. And the cancer cell lines, SMMC-7721 and MCF7, were the most sensitive, with MCF7

exhibiting the fastest kinetics to cell death.

In addition to the variable sensitivity to primary NK cell killing, the different target cell types also showed cell death response through distinct cytotoxic pathways (Figure 4.1B). About 60% cell death seen in target cell, SMMC-7721, were preceded by a loss of the granzyme-B FRET signal that resulted in an increase of CFP signal. Loss of granzyme-B FRET was followed by MOMP, illustrated by the abrupt transition from punctate to smooth localization of the fluorescence signal from the mitochondria reporter, IMS-RP. As discussed in Chapter 3, such combined characteristics from the two fluorescent reporters suggested NK cell killing of SMMC-7721 was mainly through lytic granule-mediated apoptosis (Fig. 4.1B). Cytotoxicity against U-2 OS cells had been previously determined as being primarily mediated by death ligand, FasL, and extrinsic apoptosis, as U-2 OS cell death was preceded by MOMP, but mostly not associated with any change of the granzyme-B FRET signal (refer to the steady CFP signal in the right panel of Fig. 4.1B). Intriguingly, analysis of the target cell line panel revealed a third cytotoxic mode employed by primary NK cell. Unlike SMMC-7721 and U-2 OS, the majority of cell death observed in MCF7 cells was not preceded by MOMP, indicating it was not classic apoptosis. Moreover, signal from the granzyme-B FRET reporter was abruptly lost upon extensive MCF7 cell blebbing, pointing to large-scale leakage of intracellular content likely due to membrane ruptures. Such dynamic features were consistent with necrotic cell death, whose relevance in NK cell cytotoxicity is largely uncharacterized.

Figure 4.1C summarized the percentage of live target cells and the cell death population through the three distinct cytotoxic mechanisms of primary NK cell in the

five target cell lines, including lytic granule-mediated apoptosis, death ligand-mediated apoptosis and necrosis after 12 hours of NK-target cell co-culture. The two most sensitive target cell lines, SMMC-7721 and MCF7, which showed rapid kinetics of cell death induction, were killed mainly (around 60%) through lytic granule or necrosis, while cytotoxicity mediated by death ligand on NK cell surface was more dominant towards the less sensitive target cell types, U-2 OS, HeLa and LO2. This implied cytotoxic dynamics induced by lytic granule and necrosis were faster than that by death ligand and that target cells susceptible to these two cytotoxic modes can be eliminated by NK cell more effectively. Moreover, all target cell lines showed substantial cell death triggered by death ligand of NK cell, ranging from 23% to 57% of the total target cell population. In contrast, the extent of cell death activated by lytic granule and necrosis varied more significantly between the different target cell lines, ranging from 1% to 54% for the lytic granule mode and 1% to 57% for the necrotic mode. Such large variability in sensitivity to NK cell killing by lytic granule and necrosis indicated activation of these two cytotoxic modes was highly specific to target cell types.

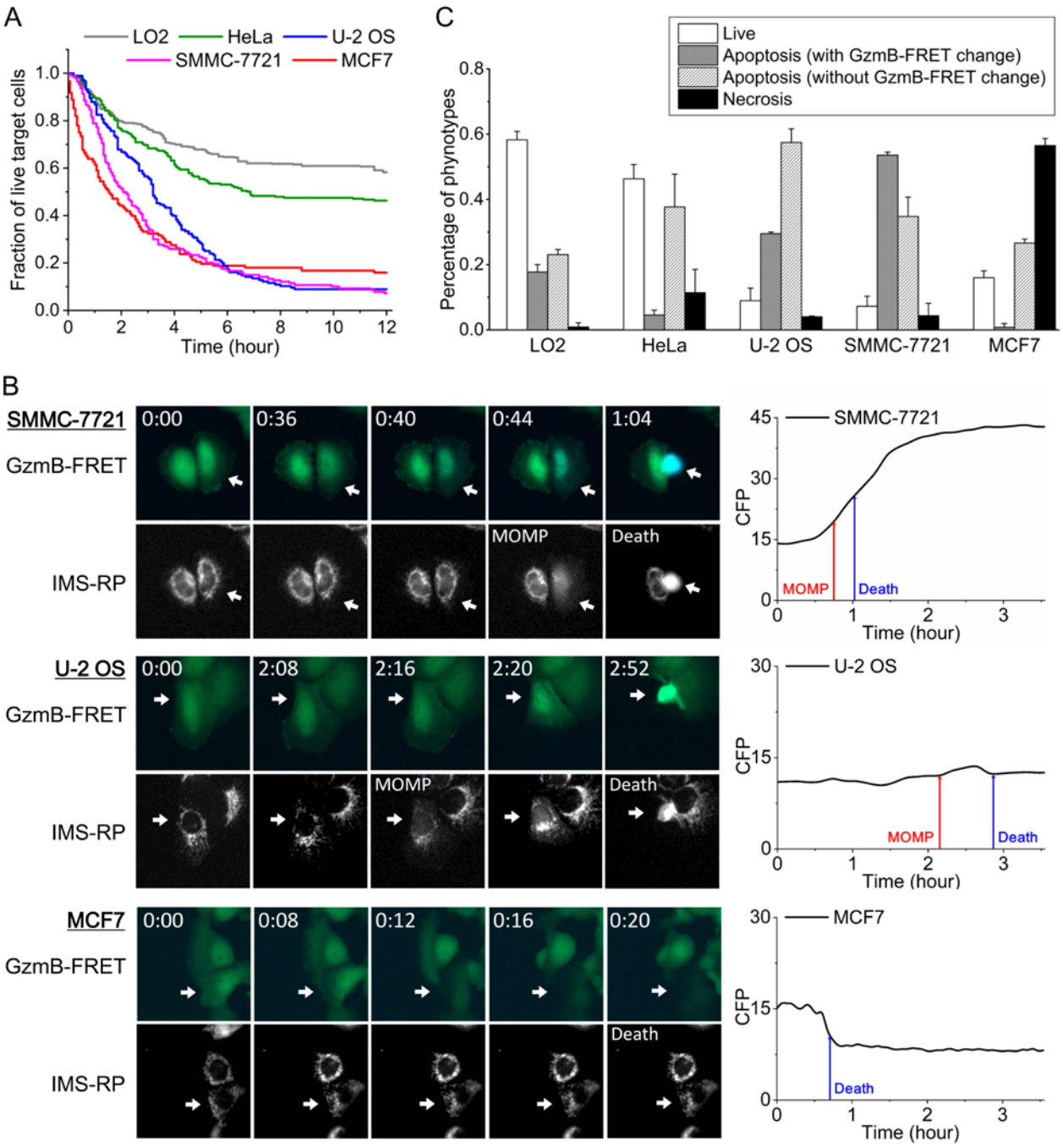

Figure 4.1. Characteristics of cytotoxic dynamics of primary NK cell against five different target cell lines. (A) Cumulative survival curves of target cells, including LO2 (denoted in grey), HeLa (green), U-2 OS (blue), SMMC-7721 (magenta) and MCF7 (red), under co-culture with primary NK cell at a NK-to-target cell ratio of 3:1. For all co-

culture experiments, 50 ng/ml IL-2 was supplemented in the medium. Individual target cells were monitored by phase-contrast and fluorescent time-lapse microscopy, and time from NK cell addition to morphological target cell death was analyzed and plotted as cumulative survival curves. Data were averaged from 2 independent imaging experiments and the number of cells analyzed ranges from 40 to 223, varied between experiments and target cell lines. (B) Left panels: Fluorescent images of the granzyme-B (GzmB) FRET reporter and the corresponding mitochondria reporter, IMS-RP, from SMMC-7721, U-2 OS and MCF7. The GzmB-FRET images are overlay of the CFP (denoted by blue) and YFP (denoted by green) channels. Time (unit: hour:minute) is indicated at the top left corner of each GzmB-FRET image. Right panels: Representative single cell trajectories of CFP signal quantified by monitoring CFP fluorescence over time for the above three target cell lines. The time of MOMP, scored by IMS-RP signal, is indicated by the red vertical line. And the time of death, scored morphologically by cell blebbing and lysis, is indicated by the blue vertical line. (C) Distributions of live and dead target cells killed by the three distinct cytotoxic mechanisms of primary NK cells after 12 hours of co-culture, as discussed in the text. Data were averaged from 2 independent imaging experiments and the error bars indicate standard deviations.

4.2 Mechanism of necrotic death induced by primary NK cell

As necrotic death is associated with membrane rupture, I hypothesized that membrane pores formed by perforin at the NK-target cell conjugation may be involved in triggering the necrotic death and membrane rupture. To examine the role of perforin in the necrotic mode of NK cell cytotoxicity, I pre-treated primary NK cells with Concanamycin A (CMA), an inhibitor of perforin, at saturating dosage (1 μM), and then co-cultured the NK cells with MCF7 cells, the target cell line that showed high level of necrotic death in the presence of primary NK cells (CMA was included in the co-culture medium to maintain perforin inhibition). As shown in Figure 4.2A and 4.2B, the presence of CMA significantly attenuated MCF7 cell death induced by primary NK cells, and the reduction in overall target MCF7 cell death was mostly due to the decrease of necrotic death, which decreased from 52% to 4% of the target cell population after 12 hours of co-culture. This result illustrated a key role played by perforin in mediating the necrotic cytotoxicity of primary NK cells.

Given that lytic granule-mediated cytotoxicity of NK cells and necrotic death are both mediated by perforin, it is unclear how these two cytotoxic modes could be differentially activated by the same NK cells towards different target cell types, e.g., SMMC-7721 vs. MCF7. A simple possibility is that perforin may form pores of different sizes, depending on the target cell characteristics. For small pores, granzyme-B could be released without significant disruption of the target cell membrane, thus allowing the more controlled apoptosis to occur. In contrast, If the pores are large, target cell membrane would rupture, leading to necrotic death. To test this hypothesis, I performed a dose titration of CMA to partially inhibit perforin, thus potentially reducing the pore

sizes in MCF7 cells, and examined effect on the extent of necrosis and lytic granule-mediated apoptosis induced by primary NK cells. I found 4 to 5 nM CMA partially inhibited the degree of necrotic death in MCF7 cells, i.e., from about 60% to 30%, indicating perforin activity was partially inhibited at this dosage. Interestingly, the decrease in necrotic death was accompanied by an evident increase of lytic-granule-mediated apoptosis (from 5% to 20%), demonstrating that partial inhibition of perforin in MCF7 cells promoted lytic-granule-mediated cytotoxicity of primary NK cells, likely due to the reduction in membrane pore size. Further studies, such as by super-resolution imaging of the perforin pores at NK-target cell conjugation, are needed to confirm this result and elucidate the underlying dynamic mechanisms.

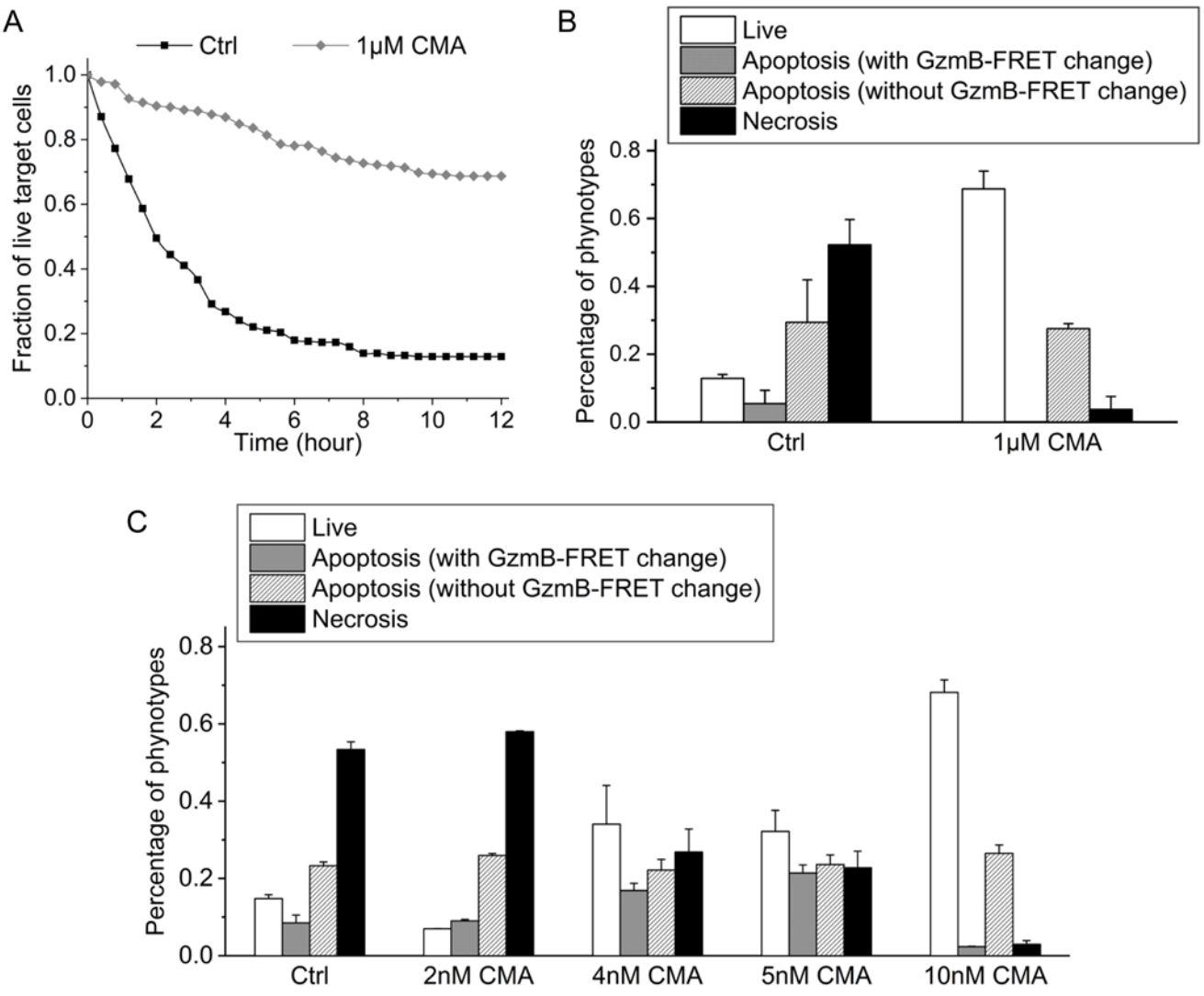

Figure 4.2. Necrotic death induced by primary NK cells is likely due to large membrane pores formed by perforin. (A) Cumulative survival curves of MCF7 cells after 12 hours of co-culture with primary NK cells (3-day cultured in IL-2) at NK-to-target cell ratio of 3:1 under control condition or in the presence of 1 μM Concanamycin A (CMA). Data were averaged from 2 independent imaging experiments and the number of cells analyzed ranges from 73 to 149. (B) Distributions of live and dead MCF7 cells killed by the three distinct cytotoxic mechanisms of primary NK cells under the indicated

treatment condition. Data were averaged from 2 independent imaging experiments and the error bars indicate standard deviations. (C) Distribution of the live and dead MCF7 cells after 12 hours of co-culture with primary NK cells as a function of CMA concentration.

4.3 Target specificity of NK cell cytotoxic activity on inhibitory and activating NK cell receptors

As my data showed highly variable sensitivity of different target cell lines to the three cytotoxic modes of primary NK cell, a crucial mechanistic question is what controls the target specificity of NK cell cytotoxicity. As discussed in the Introduction, NK-target cell interactions are primarily regulated by collective signaling from multiple inhibitory and activating receptors on NK cell surface. To determine how individual as well as combination of these receptors contribute to NK cell cytotoxic activity against distinct target cell types and pinpoint receptors associated with particular cytotoxic modes and kinetics, I used neutralizing antibodies to block NK-target cell interaction through specific inhibitory or activating receptor(s), and then compared the extent and kinetics of target cell death with those under the control condition. Specifically, I examined the potential functional involvement of two types of inhibitory receptors, KIRs and NKG2A (CD94), and three activating receptors that are important for cancer target recognition, including NKG2D (CD314), DNAM-1 (CD226) and NKp46 (CD335)[44,46–49]. As there are several KIRs that recognize different HLA molecules on target cell surface, to simplify the analysis I used a broad-spectrum neutralizing antibody against HLA-A, -B and -C on target cell surface to block interaction of all KIRs and human MHCI molecules as a whole, instead of examining the individual KIR.

To take HeLa cells as an example, as expected, blocking the inhibitory NK-HeLa cell interaction via both MHCI molecules and NKG2A accelerated and enhanced HeLa cell killing by primary NK cell, with MHCI neutralization showing a stronger effect (Fig. 4.3A). Moreover, simultaneous blockage of MHCI molecules and NKG2A further

increased NK cell cytotoxic activity towards HeLa cells, resulting in a degree of cell death similar to that observed in the sensitive target cell lines, such as SMMC-7721. Neutralizing the activating receptors on NK cell exerted less prominent effect in altering (i.e., attenuating) the cell death response of HeLa, possibly due to the fact that HeLa cells under control condition (i.e., no perturbation of receptor activity) are already relatively resistant to primary NK cell killing. Inhibition of NKG2D activity exhibited a stronger effect in attenuating HeLa cell death than neutralizing DNAM-1 or NKp46 (Fig. 4.3B). Double blocking of NKG2D plus DNAM-1 or NKp46 further rescued HeLa cell death induced by primary NK cells, confirming that the cytotoxic dynamics of primary NK cells were regulated by collective, rather than individual, signaling receptors. In terms of potential differential role of the receptors in modulating the three distinct cytotoxic modes of primary NK cell, my results did not show obvious receptor-specific effect that correlated with the cytotoxic mode. Percentages of NK cell killing mediated by lytic granule, death ligand and necrosis all increased upon blockage of the inhibitory interaction between KIRs and MHCI molecules on HeLa cells, and decreased upon neutralizing NKG2D alone or in combination with DNAM-1 or NKp46 (except the necrotic population) (Fig. 4.3C), pointing to more complex mechanism(s) that determines the specificity of cytotoxic mode of primary NK cell.

To further examine variable receptor dependence of NK-target cell interaction in the five target cell lines, I plotted percentages of the live as well as dead target cells killed by the three cytotoxic modes under different receptor neutralization conditions relative to those of control, i.e., no receptor blockage, in Figure 4.3D. Intuitively, data points along the diagonal indicated no change relative to the control condition, and the further away

the data points were from the diagonal, the larger the effect of the particular receptor inhibition was to alter the cell death response to NK cell cytotoxicity. Similar to HeLa, neutralization of the inhibitory KIRs-MHCI interaction exerted stronger effect than blocking NKG2A in enhancing cell death response of the other four target cell lines, and loss of NKG2D activity exerted the strongest effect among the three activating receptors in attenuating target cell death. Double inhibition of NKG2D and DNAM-1 nearly blocked cell death response of target cell lines that are sensitive to primary NK cell killing, including U-2 OS, SMMC-7721 and MCF7. Given that these three cell lines died through distinct cytotoxic pathways, the activating receptors, NKG2D and DNAM-1, alone were unlikely to confer target specificity of NK cell in terms of the cytotoxic mechanism. Nonetheless, perturbing the NK cell receptors (both inhibitory and activating) did appear to alter cell death response of the different target cell lines through one particular cytotoxic mode, illustrated by the large vertical spread of data away from the diagonal in Fig. 4.3D, including lytic granule-mediated death for SMMC-7721, death ligand-mediated death for HeLa and to a lesser extent for LO2 and U-2 OS, and necrotic death for MCF7. I therefore think my data still argued for the presence of target-specific mechanism in activating a particular cytotoxic mode of primary NK cell, although the receptor-ligand blocking analysis did not identify any well-known NK receptor that renders such target specificity.

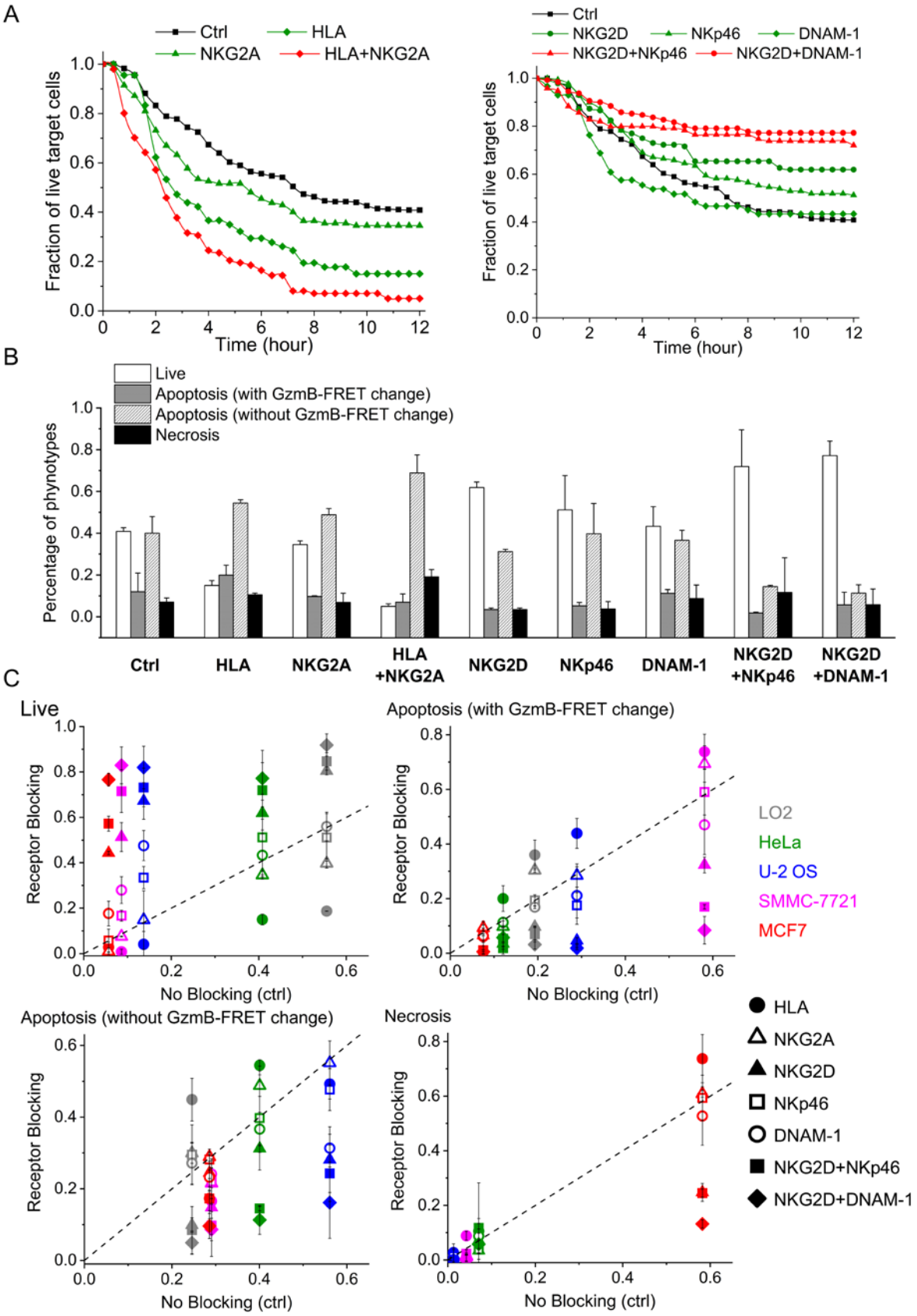
A
Ctrl
HLA
NKG2A
HLA+NKG2A
Fraction of live target cells
Time (hour)
Ctrl
NKG2D
NKp46
DNAM-1
NKG2D+NKp46
NKG2D+DNAM-1
Fraction of live target cells
Time (hour)
B
Live
Apoptosis (with GzmB-FRET change)
Apoptosis (without GzmB-FRET change)
Necrosis
Percentage of phynotypes
Ctrl
HLA
NKG2A
HLA +NKG2A
NKG2D
NKp46
DNAM-1
NKG2D +NKp46
NKG2D +DNAM-1
C
Live
Apoptosis (with GzmB-FRET change)
Apoptosis (without GzmB-FRET change)
Necrosis
Receptor Blocking
No Blocking (ctrl)
LO2
HeLa
U-2 OS
SMMC-7721
MCF7
HLA
NKG2A
NKG2D
NKp46
DNAM-1
NKG2D+NKp46
NKG2D+DNAM-1

Figure 4.3. Blocking inhibitory and activating receptors of primary NK cells showed differential effect on altering cell death response of the five target cell lines. (A) Cumulative survival curves of HeLa cells in co-culture with primary NK cell in the presence of single or double inhibitory receptor blocking (left panel) or activating receptor blocking (right panel). (B) Distributions of live and dead HeLa cells killed by the three distinct cytotoxic modes of primary NK cells after 12 hours of co-culture under the indicated blocking conditions. Data were averaged from 2 or 3 independent imaging experiments and the error bars indicate standard deviations. (C) Percentage of live cells (upper left panel) and cells dying through lytic granule (with FRET signal loss, upper right panel), death ligand (without FRET signal loss, lower left panel) and necrosis (lower right panel) under different receptor blocking conditions in comparison with those under the control condition. Data from the five target cell lines were color coded as follows, LO2 in gray, HeLa in green, U-2 OS in blue, SMMC-7221 in magenta and MCF7 in red. The different single and double receptor blocking were denoted with the indicated symbols.

4.4 Differential expression of activating and inhibitory ligands on target cells

To explore other potential regulators involved in rendering the target specificity of primary NK cell, I next examined the levels of various activating and inhibitory ligands expressed by the different target cell types on cell surface. The same inhibitory/activating NK cell receptor is known to interact with multiple ligands, for instance, the NKG2D activating receptor interacts with a number of cancer-associated NKG2D ligands, including MICA, MICB and different ULBPs[46,51,82,90,118]. It is thus possible that the target specificity is determined by the identity and level of a subset of activating and/or inhibitory ligands recognized by the NK cell receptor(s). Since neutralizing KIRs-MHCI interaction as well as NKG2D exhibited the strongest effect in altering target cell death induced by NK cell for all five target cell lines, human MHCI molecule, HLA-A,B,C, and NKG2D ligands, including MICA, MICB and ULBP-2,5,6, were chosen for the surface expression profiling analysis. In the analysis panel, I also included activating ligands for DNAM-1, including CD155 and CD112, as blocking DNAM-1 also notably attenuated NK cell killing, as well as the death receptor Fas and an integrin key for NK cell adhesion, ICAM-1 (CD54). The above ligands were stained with their respective fluorescent dye-conjugated primary antibodies and expression was then measured by flow cytometry (Fig. 4.4A).

Quantification of the flow cytometry data showed variable sensitivity of the target cell lines to overall NK cell killing correlated well with the expression level of the inhibitory MHCI molecules, and to a lesser extent with MICB, but did not correlate with expression of the other NKG2D activating ligands, MICA and ULBPs, or the activating ligands for DNAM-1 (Fig. 4.4B). This suggested that the inhibitory strength between

KIRs of NK cells and MHCI molecules of the targets may provide the primary signal to modulate NK cell cytotoxicity against a particular target. However, the data again did not show any obvious correlative feature specific to the three distinct cytotoxic modes of primary NK cell. The only differential ligand expression that may potentially render specificity to necrotic killing is MICB. The MICB expression level in MCF7, a target cell line that was particularly prone to necrotic death, was 5-10 folds higher than that observed in the other four cell lines. The strong activating signal from MICB may facilitate formation of large perforin pores in the MCF7 cell membrane, thus leading to necrosis. This hypothesis clearly requires further investigation, e.g., with MICB-specific neutralizing antibody.

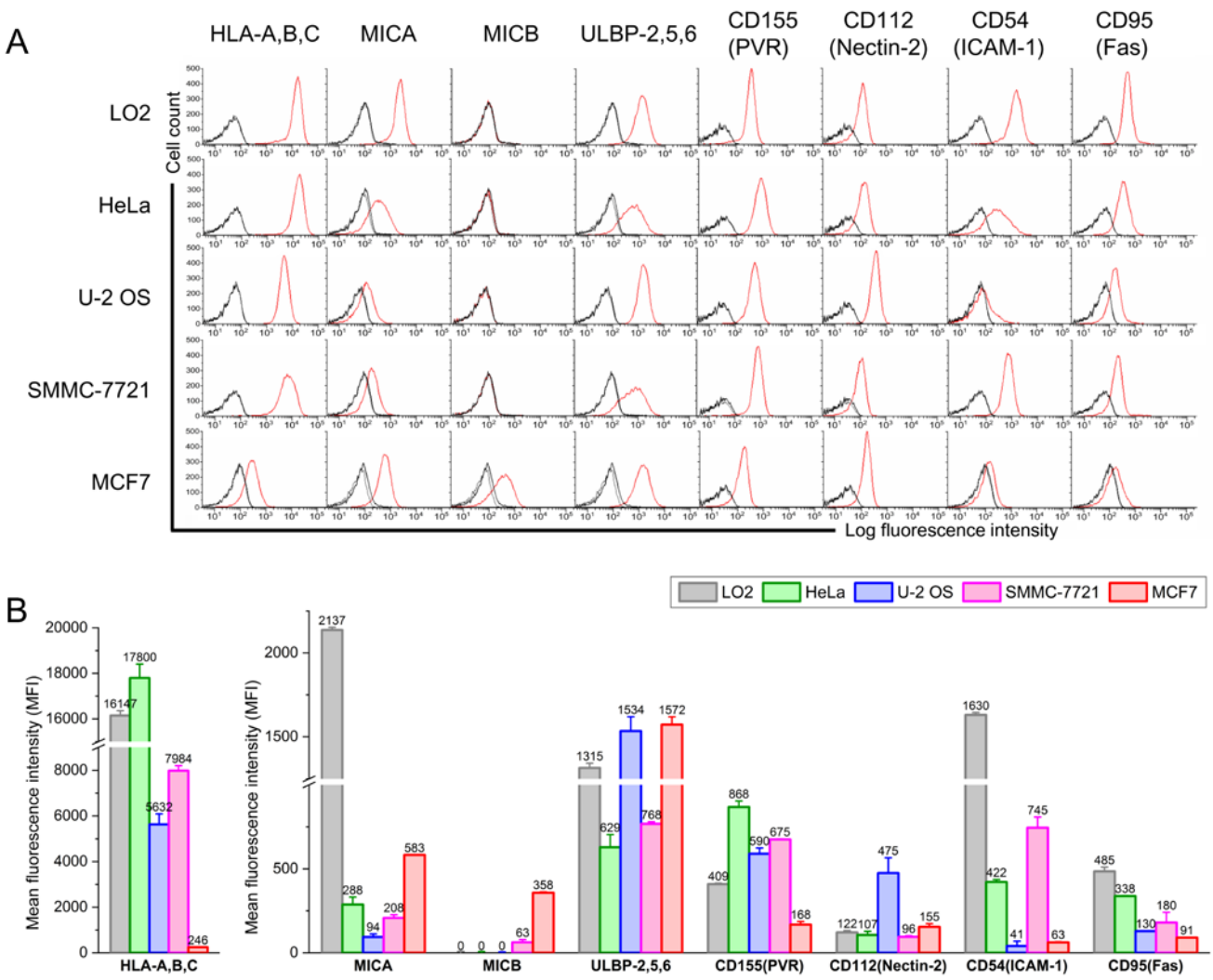

Figure 4.4. The five target cell lines expressed variable levels of NK cell activating and inhibitory ligands as well as Fas and integrin, ICAM-1, on cell surface. (A) Flow cytometry analysis of expressions of the selected surface proteins by staining with dye-conjugated antibody specific to the protein (red curves) in comparison with dye-conjugated, non-specific isotope control (black curves). (B) Comparison of the surface protein expression in the five target cell lines based on the average florescence signal from flow cytometry analysis of each protein staining. Cell lines were color coded as indicated. Data were averaged from 2 independent flow cytometry analyses (>1×10^4 cells were counted in each analysis) and error bars are standard deviations.

Chapter 5 Discussion and Conclusion

By simultaneously monitoring and quantifying the real-time dynamics of multiple cytotoxic pathways that contribute to NK-target cell interaction, my PhD study pinpointed, at the single cell level, how activation of the distinct cytotoxic modes of primary human NK cell, including lytic granule-mediated apoptosis, death ligand-mediated apoptosis and necrosis, varies kinetically and against different target cell types, thus resulting in killing heterogeneity. The strong contribution that I observed from non-lytic granule-mediated cytotoxicity, e.g., through FasL and necrosis, came as an unexpected result, as most NK cell studies in the literature reported on the dominant role of the lytic granule-mediated pathway. For the two less well-known cytotoxic modes of NK cell, my data revealed interesting new dynamic features and their associated regulatory mechanisms. For instance, I found that the death ligand signaling pathway not only directly triggers cancer cell death but also sensitizes some cancer cell, such as U-2 OS, to cytotoxicity induced by lytic granule. Moreover, cytotoxicity triggered by the FasL pathway outweighs the lytic granule mechanism even more, under low NK-to-target cell ratio (i.e., 2:1 as compared to 5:1) and low level of activating cytokine, IL-2, conditions probably closer to *in vivo* situation, indicating that the death ligand-mediated mechanism may play a major role in exerting cytotoxicity for some target cell types *in vivo*. Extensive necrotic death was only observed in MCF7 cells, with rapid kinetics of cell death induction similar to lytic granule-mediated killing. Given the relatively low level of necrotic death in the other three target cancer cell lines that I studied, it is unclear whether the necrotic pathway is as physiologically relevant as the other two cytotoxic

modes in mediating primary NK cell activity. Overall, although my findings need to be further examined and validated using animal model, they still point to potentially important role of the non-lytic granule pathways in regulating the cytotoxicity of primary NK cell, which should be taken more into consideration, e.g., in the development of NK cell therapy. A recent study revealed an intricate control of tumor growth by NK cell uniquely through the FasL mechanism[119], suggesting that the FasL mechanism may indeed be exploited to provide new targets and strategies for engineering primary NK cells for adoptive cell transfer therapy.

In order to further investigate whether the three distinct cytotoxic modes are physiologically relevant to the real tumor immune defense *in vivo*, analysis of primary NK cell cytotoxic activity against 3D primary tumor organoids may be performed. The recent advances in 3D primary tumor organoid culture provide a new, and more physiologically relevant 3D tumor system to understand immune and tumor cell interactions[120–122]. By conducting the single cell imaging assays with co-culture of primary NK cells and 3D tumor organoids, it would likely reveal new dynamic insight towards understanding how the three different cytotoxic modes contribute to tumor cell elimination in a complex 3D tumor microenvironment.

Moreover, as discussed above, extensive necrotic death was only observed in MCF7 cells and the other three target cancer cell lines that I studied only exhibited relatively low level of necrotic death. This raises important question regarding the particular molecular and cellular characteristics that make MCF7 cells especially susceptible to die through necrosis upon interacting with primary NK cells. Based on results demonstrated in Chapter 4.2, investigating whether the pore size truly determines the choice of

cytotoxic modes made by MCF7 as well as quantifying the exact pore size that triggers necrosis will provide data to shed light on the activating signal for necrotic killing of MCF7 cells and other cancer target that harbors the same characteristics. Possible experiment includes using propidium iodide (PI) to first examine membrane leakage as a surrogate for pore formation on the MCF7 membrane before necrosis[56]. If accumulation of PI fluorescence is observed in the cytoplasm of the MCF7 cell prior to cell death, it will confirm my results obtained with the titration of perforin inhibitor CMA as discussed in chapter 4.2, and also confirm that the membrane pore formed before MCF7 necrosis and the observed necrosis is mediated by perforin and cytolytic granule. In addition, as necrosis induced by NK cells exhibited the fastest killing kinetics among the three cytotoxic modes, completing in only several minutes, in order to monitor the real-time dynamics of pore formation one would need high speed and high resolution microscope system, such as the light sheet fluorescence microscopy (LSFM). I believe light-sheet imaging will provide new dynamic insight regarding the mechanism of pore formation that led to necrotic MCF7 cells upon interaction with primary NK cells.

As the majority of target cells died after multiple interactions with the primary NK cells, and also that not all NK-target contacts led to target cell death, it raised an important question of what distinguishes the cytotoxic and non-cytotoxic contacts between NK and target cells. To acquire data on NK-target contact truly at the single cell level, the current bulk assay, i.e. co-cultures of a large number of NK cells with target cells, is deemed not suitable, as it is extremely difficult to track single NK cells when a large number of them move quickly in the field of view. The application of microfluidic chips, such as arrays of polydimethylsiloxane (PDMS) nanowell columns of 50-100 μm,

would be a good platform to encage single target cell with different number of NK cells (e.g., 1 to 5) and allow measurement of the NK-target interaction dynamics at the single cell level. PDMS is a biocompatible, nontoxic, transparent and non-fluorescent material, thus widely used for fabrication of microfluidic devices[123,124]. Some previous studies have already used microfluidic chips to investigate NK-target cell interaction dynamics. For instance, Björn Önfelt et al. illustrated that NK-target cell interaction dynamics could be scored and statistically quantified at single cell level by live-cell imaging with multi-well microstructures[93]. They further utilized this multi-well microstructures technique to examine how the NK cell cytotoxicity, migration behavior, and NK-target cell interaction dynamics were affected by NK cell activating cytokines as well as expression levels of specific surface markers, such as KIRs and NKG2A etc[125,126]. Martin Wiklund et al. used a different design involving a sandwich-type microplate consisting one glass layer, one silicon layer and one PDMS layer. With the microplate device they characterized the 3D tumor structure with a culture cancer cell line HepG2 and monitored the migration and interaction dynamics of primary NK cells with the 3D tumor model[127]. Prof. S. Pang's research group at the City University of Hong Kong also developed a microwell arrays with microchannel connections in PDMS substrates to study the NK-cancer cell interaction dynamics in a confined microenvironment[128]. Overall, inspired by these previous studies, in the future study the microfluidic chips with confined microenvironment will provide a very useful imaging platform to acquired more quantitative single cell data towards better understanding of the cytotoxic dynamics of NK cell towards distinct cancer target.

In collaboration with Prof. S. Pang, prototypes of some possible PDMS chips for the

future single cell analysis have been fabricated. Figure 5.1 illustrates several examples of the PDMS chip designs. The arrays of PDMS nanowell columns of 50-150 μm (Fig.5.1 A1-A3) were designed to encage single target cancer cell with up to five primary NK cells. With this PDMS nanowell chips, the NK-cancer cell interaction dynamics can be easily quantified at defined NK-to-target cell ratio. It is also possibl to employ the microfluidic platform to investigate dynamics of NK cell polarization and motility. The process of NK cell polarization and migration are known to be crucial for its activity, as NK cell polarization engenders the proper orientation for forming NK-target immunological synapse and also increases NK cell motility. NK cell motility is also believed to be the most critical factor in determining NK cell cytotoxicity towards tumor *in vivo*. To perform real-time tracking and quantification of NK cell polarization and motility, PDMS chips with distinct nanowells linked by channels of 5-10 μm width or different linkage shapes were designed (Fig.5.1 B and C). The different linkage sizes and shapes will allow me to examine how physical geometry affects NK cell motility both in terms of directionality and velocity in the presence vs. absence of target cell in the opposite reservoir. Moreover, it could be also a good idea to utilize simple one-dimensional microfluidic channels of various widths to measure NK cell motility in response to defined cytokine or chemokine gradient (Fig.5.1 D). I can place primary NK cells at one end of the channel, then inject cytokine or chemokine that is known to activate NK cell activity (e.g., IL-2 and IL-15) through the other end of the channel, and then analyze the dynamics of NK cell polarization and motility in comparison with NK cell alone (without extra cytokine/chemokine) and NK cell in co-culture with target cancer cells. The combined data from the chip-assisted single cell analysis will allow me

to identify and quantify dynamic parameters underlying NK cell polarization and motility, and determine how alterations in specific micro-environmental parameters contribute to changes in NK cell migration towards the cancer targets.

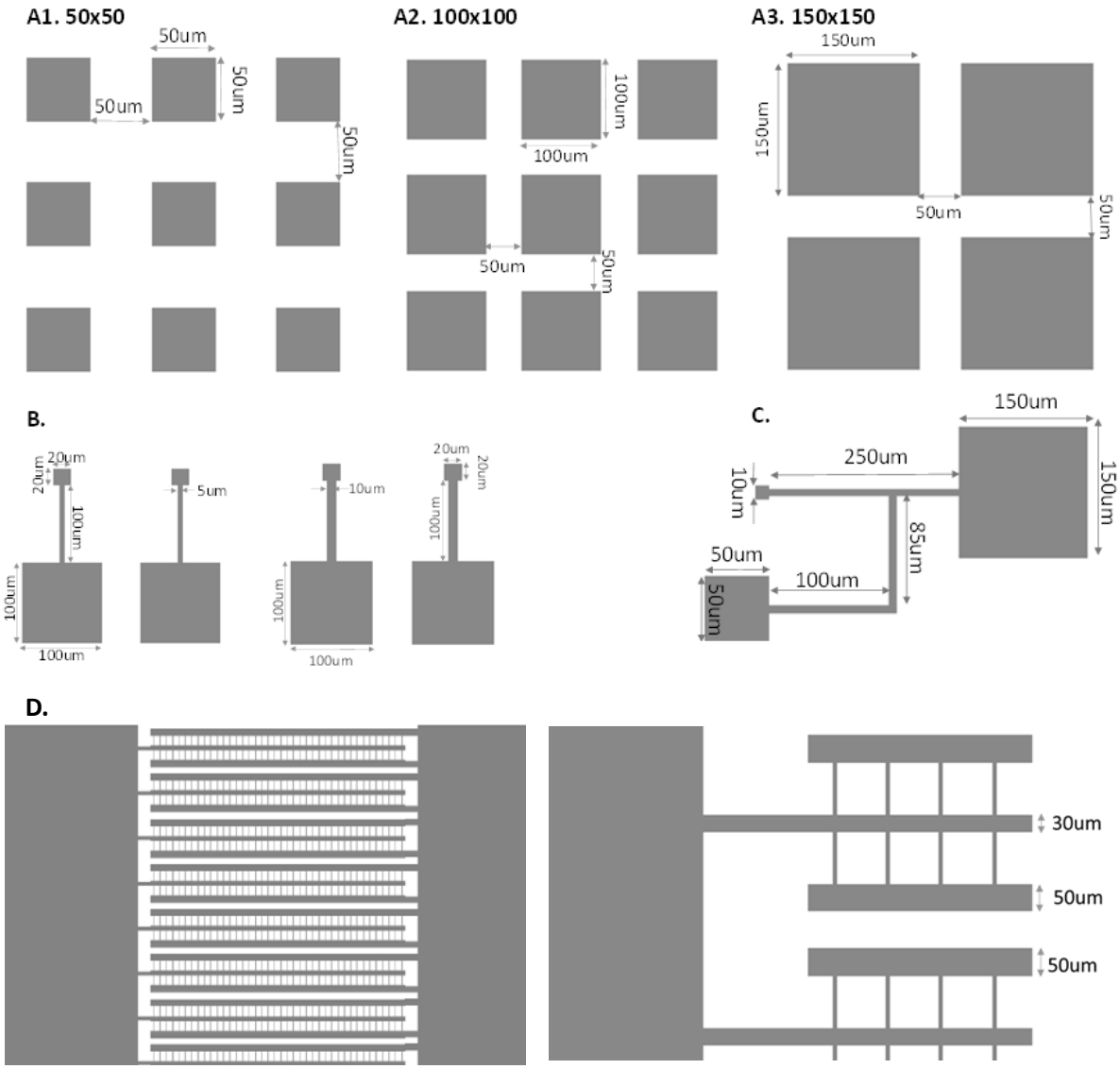

Figure 5.1. Examples of some design sketches of the PDMS chips. (A1-3) PDMS chips with nanowells in different size; (B) and (C) PDMS chips with different sizes of nanowells linked by 5-10 μm width channels in different length or different linkage shapes; (D) PDMS chips with channels linking the two pools. The right one is the full view structure of the chips, and the left one is with an enlarged scale.

Sensitivity of different target cell lines to primary NK cell killing was found to depend on and best correlate with the expression level of MHCI molecules on the target cell surface for both normal and cancer targets, indicating that the inhibitory strength between KIRs on NK cell and MHCI on target cells likely plays a key regulatory role. Surprisingly, I observed very high level of activating NKG2D ligands, such as MICA and ULBPs, on the normal cell line, LO2, which was contradictory to LO2's resistance to NK cell killing and the common hypothesis that over-expression of NKG2D ligands are particularly associated with transformed tumor cells. This result has two implications. Firstly, it puts a cautious note on using NKG2D ligands to predict target sensitivity to NK cell therapy, as proposed by previous studies based on correlative analysis with mostly cancer cell lines[76,83–85,92,118,129,130]. Secondly, it accentuates the importance of collective signaling from multiple inhibitory and activating receptor-ligand interactions in determining the overall NK cell cytotoxicity against a target cell type. It is not yet clear how the individual receptor-ligand interactions quantitatively contribute to the collective activation signal, e.g., whether the signaling is simply additive or has differential dependence on particular receptor-ligand interaction. Both experimental and computational analyses are needed in order to characterize and quantify the multi-signaling mechanism at the system level, which shall improve prediction of target sensitivity to NK cell killing, e.g., for cancer patients that may receive adoptive cell transfer therapy.

Although the single cell data elucidated the differential rate-limiting kinetics associated with the three cytotoxic modes of primary NK cell, they fell short of identifying regulatory components/interactions that engender the target specificity of

these distinct cytotoxic pathways. The only potential correlate that I found specifically with necrotic death in MCF7 cells is surface expression level of MICB. Neutralizing antibody specific to MICB should be used in follow-up studies to test the functional contribution of MICB to the necrotic mode of primary NK cells. In a broader sense, the lack of obvious receptor-ligand interaction in regulating a particular cytotoxic signaling pathway may be due to the limited number of NK cell receptors and target ligands that were analyzed, or that the specificity is rendered by differential localization of the activating and inhibitory ligands on the target cell surface, rather than their expression levels. Another possibility is that target specificity is controlled by more complex mechanism beyond receptor-ligand interaction, e.g., by cytokine(s) secreted by NK cells upon recognition of the different target cell types, such as TNF-α and IFN-γ. Further study is clearly needed to explore the molecular and cellular mechanism underlying the target specificity of NK cell cytotoxic activity. Nonetheless, irrespective of the precise mechanism for target specificity, an important perspective from my PhD study is that primary human NK cells exerts cytotoxicity by multiple signaling pathways; and that these distinct cytotoxic modes occur simultaneously via differential kinetics, resulting in significant dynamic heterogeneity of NK cell activity and target-specific variability.

In my study, I treated the primary NK cells as largely a homogeneous population. However, it is possible that the NK cell prep may contain NK cells of different cytotoxic capacity. To examine whether heterogeneity of NK cell populations differentially contributes to the three cytotoxic modes that I observed, in the future study, FACS sorting of the primary NK cells with specific surface marker to acquire different subsets of primary NK cells and then analyzing their respective cytotoxic dynamics towards the

five model target cell lines should be performed. Meanwhile, my data regarding the dependence of NK cell cytotoxic activity on different inhibitory and activating NK cell receptors suggested the presence of target-specific mechanism in activating a particular cytotoxic mode of primary NK cell. The reason why my data were unable to pinpoint their specific identify may be due to the possibility that the underlying specific immune checkpoint molecules are from a particular subsets of NK cells. By conducting the FACS sorting and then the receptor blocking imaging assays with the different subsets of primary NK cells, the molecular determinants for the distinct cytotoxic modes may be revealed. Elucidating the immune checkpoint molecules underlying specific cytotoxic modes of primary NK cell against different cancer type shall provide crucial new insight for developing more effective NK cell therapy for a broad spectrum of tumors.

In addition to the cytotoxic mechanisms of primary NK cell, my data also revealed new kinetic feature in the NK-target cell interaction process. For instance, the live-cell imaging results illustrated that not all transient NK-cancer cell interactions that were not immediately followed by target cell death were functionally futile, as some of them were successful FasL-Fas conjugations that led to caspase-8 activation. However, questions remain what kinetic and phenotypic determinants distinguish the FasL-Fas conjugations from most transient NK-cancer cell interactions that did not activate caspase-8. The receptor neutralization experiments showed that loss of the inhibitory KIRs-MHCI interaction significantly enhanced death ligand-mediated cell death in HeLa cells, and loss of the activating receptors, NKG2D and DNAM-1, strongly reduced death ligand-mediated death in U-2 OS cells. These data demonstrated that in addition to the death ligands on NK cells, the inhibitory and activating receptors also participate in

constraining or facilitating the death ligand-mediated cytotoxic signaling, most likely through modulating the FasL-Fas conjugation at the NK-target cell juncture. As individual primary NK cells may carry different amount of inhibitory and activating receptors, they would have variable capability to detect and interact with the target cell. Therefore, only transient interactions with a highly target-sensitive NK cell would lead to formation of FasL-Fas conjugation and subsequently activate caspase-8 and target cell death. Further study to unravel the specific molecular regulators of FasL-Fas conjugation, e.g., by simultaneously monitoring the FRET reporter and fluorescent reporter of distinct surface receptors, is needed to improve our mechanistic understanding of the dynamic control mediated by FasL signaling, and identify better cellular targets for engineering NK cells with enhanced killing efficacy.

References

1. Robertson, M. J. & Ritz, J. Biology and clinical relevance of human natural killer cells. *Blood* **76,** 2421–2438 (1990).
2. Coico, R. & Sunshine, G. *Immunology: A Short Course*. (John Wiley & Sons, 2015).
3. Stobo, J. D., Rosenthal, A. S. & Paul, W. E. FUNCTIONAL HETEROGENEITY OF MURINE LYMPHOID CELLS. *J. Exp. Med.* **138,** 71–88 (1973).
4. Greenberg, A. H. & Playfair, J. H. Spontaneously arising cytotoxicity to the P-815-Y mastocytoma in NZB mice. *Clin. Exp. Immunol.* **16,** 99–109 (1974).
5. Kiessling, R., Klein, E., Pross, H. & Wigzell, H. „Natural" killer cells in the mouse. II. Cytotoxic cells with specificity for mouse Moloney leukemia cells. Characteristics of the killer cell. *Eur. J. Immunol.* **5,** 117–121 (1975).
6. Kiessling, R., Klein, E. & Wigzell, H. „Natural" killer cells in the mouse. I. Cytotoxic cells with specificity for mouse Moloney leukemia cells. Specificity and distribution according to genotype. *Eur. J. Immunol.* **5,** 112–117 (1975).
7. Glimcher, L., Shen, F. W. & Cantor, H. Identification of a cell-surface antigen selectively expressed on the natural killer cell. *J. Exp. Med.* **145,** 1–9 (1977).
8. Vivier, E. *et al.* Innate or Adaptive Immunity? The Example of Natural Killer Cells. *Science* **331,** 44–49 (2011).
9. Pross, H. & Jondal, M. SPONTANEOUS CYTOTOXIC ACTIVITY AS A TEST OF HUMAN LYMPHOCYTE FUNCTION. *The Lancet* **305,** 335–336 (1975).

10. Vries, J. E. D., Cornain, S. & Rümke, P. Cytotoxity of non-T versus T-lymphocytes from melanoma patients and healthy donors on short- and long-term cultured melanoma cells. *Int. J. Cancer* **14,** 427–434 (1974).

11. Takasugi, M., Akira, D. & Kinoshita, K. Granulocytes as Effectors in Cell-mediated Cytotoxicity of Adherent Target Cells. *Cancer Res.* **35,** 2169–2176 (1975).

12. Kiuchi, M. & Takasugi, M. The Nonselective Cytotoxic Cell (N Cell). *JNCI J. Natl. Cancer Inst.* **56,** 575–582 (1976).

13. Nunn, M. E., Djeu, J. Y., Glaser, M., Lavrin, D. H. & Herberman, R. B. Natural Cytotoxic Reactivity of Rat Lymphocytes Against Syngeneic Gross Virus-Induced Lymphoma. *JNCI J. Natl. Cancer Inst.* **56,** 393–399 (1976).

14. Shellam, G. R. Gross-virus-induced lymphoma in the rat. V. Natural cytotoxic cells are non-t cells. *Int. J. Cancer* **19,** 225–235 (1977).

15. Sendo, F., Aoki, T., Boyse, E. A. & Buafo, C. K. Natural Occurrence of Lymphocytes Showing Cytotoxic Activity to BALB/c Radiation-Induced Leukemia RL ♂ 1 Cells. *JNCI J. Natl. Cancer Inst.* **55,** 603–609 (1975).

16. West, W. H., Cannon, G. B., Kay, H. D., Bonnard, G. D. & Herberman, R. B. Natural Cytotoxic Reactivity of Human Lymphocytes Against a Myeloid Cell Line: Characterization of Effector Cells. *J. Immunol.* **118,** 355–361 (1977).

17. Kaplan, J. & Callewaert, D. M. Expression of Human T-Lymphocyte Antigens by Natural Killer Cells. *JNCI J. Natl. Cancer Inst.* **60,** 961–964 (1978).

18. Bielefeldt Ohmann, H., Davis, W. C. & Babiuk, L. A. Functional and phenotypic characteristics of bovine natural cytotoxic cells. *Immunobiology* **169,** 503–519 (1985).

19. Ulmer, A. J., Scholz, W., Ernst, M., Brandt, E. & Flad, H.-D. Isolation and Subfractionation of Human Peripheral Blood Mononuclear Cells (PBMC) by Density Gradient Centrifugation on Percoll. *Immunobiology* **166,** 238–250 (1984).

20. Magnuson, N. S., Perryman, L. E., Wyatt, C. R., Mason, P. H. & Talmadge, J. E. Large granular lymphocytes from SCID horses develop potent cytotoxic activity after treatment with human recombinant interleukin 2. *J. Immunol.* **139,** 61–67 (1987).

21. Huh, N. D., Kim, Y. B. & Amos, D. B. Natural killing (NK) and antibody-dependent cellular cytotoxicity (ADCC) in specific pathogen-free (SPF) miniature swine and germfree piglets. III. Two distinct effector cells for NK and ADCC. *J. Immunol.* **127,** 2190–2193 (1981).

22. Herberman, R. B. *et al.* Natural Killer Cells: Characteristics and Regulation of Activity. *Immunol. Rev.* **44,** 43–70 (1979).

23. Timonen, T., Herberman, R. B. & others. Characteristics of human large granular lymphocytes and relationship to natural killer and K cells. *J. Exp. Med.* **153,** 569–582 (1981).

24. Vivier, E., Tomasello, E., Baratin, M., Walzer, T. & Ugolini, S. Functions of natural killer cells. *Nat. Immunol.* **9,** 503–510 (2008).

25. Mamessier, E. *et al.* Peripheral Blood NK Cells from Breast Cancer Patients Are Tumor-Induced Composite Subsets. *J. Immunol.* **190,** 2424–2436 (2013).

26. Preethy, S. *et al.* Natural killer cells as a promising tool to tackle cancer—A review of sources, methodologies, and potentials. *Int. Rev. Immunol.* **36,** 220–232 (2017).

27. Westermann, J. & Pabst, R. Distribution of lymphocyte subsets and natural killer cells in the human body. *Clin. Investig.* **70,** 539–544 (1992).

28. Grégoire, C. *et al.* The trafficking of natural killer cells. *Immunol. Rev.* **220,** 169–182 (2007).

29. Ferlazzo, G. & Carrega, P. Natural killer cell distribution and trafficking in human tissues. *Front. Immunol.* **3,** (2012).

30. Lanier, L. L., Testi, R., Bindl, J. & Phillips, J. H. Identity of Leu-19 (CD56) leukocyte differentiation antigen and neural cell adhesion molecule. *J. Exp. Med.* **169,** 2233–2238 (1989).

31. Caligiuri, M. A. Human natural killer cells. *Blood* **112,** 461–469 (2008).

32. Autissier, P., Soulas, C., Burdo, T. H. & Williams, K. C. Immunophenotyping of lymphocyte, monocyte and dendritic cell subsets in normal rhesus macaques by 12-color flow cytometry: Clarification on DC heterogeneity. *J. Immunol. Methods* **360,** 119–128 (2010).

33. Ritz, J., Schmidt, R. E., Michon, J., Hercend, T. & Schlossman, S. F. Characterization of Functional Surface Structures on Human Natural Killer Cells. in *Advances in Immunology* (ed. Dixon, F. J.) **42,** 181–211 (Academic Press, 1988).

34. Poli, A. *et al.* CD56bright natural killer (NK) cells: an important NK cell subset. *Immunology* **126,** 458–465 (2008).

35. Milush, J. M. *et al.* CD56negCD16+NK cells are activated mature NK cells with impaired effector function during HIV-1 infection. *Retrovirology* **10,** 158 (2013).

36. Farag, S. S. & Caligiuri, M. A. Human natural killer cell development and biology. *Blood Rev.* **20,** 123–137 (2006).

37. Cooper, M. A. *et al.* Human natural killer cells: a unique innate immunoregulatory role for the CD56(bright) subset. *Blood* **97,** 3146–3151 (2001).

38. Romagnani, C. *et al.* CD56brightCD16− Killer Ig-Like Receptor− NK Cells Display Longer Telomeres and Acquire Features of CD56dim NK Cells upon Activation. *J. Immunol.* **178,** 4947–4955 (2007).

39. Chan, A. *et al.* CD56bright Human NK Cells Differentiate into CD56dim Cells: Role of Contact with Peripheral Fibroblasts. *J. Immunol.* **179,** 89–94 (2007).

40. Tseng, H.-C. *et al.* Increased Lysis of Stem Cells but Not Their Differentiated Cells by Natural Killer Cells; De-Differentiation or Reprogramming Activates NK Cells. *PLOS ONE* **5,** e11590 (2010).

41. Takahashi, E. *et al.* Induction of CD16+ CD56bright NK Cells with Antitumour Cytotoxicity not only from CD16− CD56bright NK Cells but also from CD16− CD56dim NK Cells. *Scand. J. Immunol.* **65,** 126–138 (2006).

42. Jewett, A., Cavalcanti, M. & Bonavida, B. Pivotal role of endogenous TNF-alpha in the induction of functional inactivation and apoptosis in NK cells. *J. Immunol.* **159,** 4815–4822 (1997).

43. Medzhitov, R. & Janeway, C. A. Decoding the Patterns of Self and Nonself by the Innate Immune System. *Science* **296,** 298–300 (2002).

44. Lanier, L. L. NK Cell Receptors. *Annu. Rev. Immunol.* **16,** 359–393 (1998).

45. Long, E. O. Regulation of Immune Responses Through Inhibitory Receptors. *Annu. Rev. Immunol.* **17,** 875–904 (1999).

46. Bryceson, Y. T., March, M. E., Ljunggren, H.-G. & Long, E. O. Activation, co–activation, and co–stimulation of resting human NK cells. *Immunol. Rev.* **214,** (2006).

47. Yokoyama, W. M. & Plougastel, B. F. M. Immune functions encoded by the natural killer gene complex. *Nat. Rev. Immunol.* **3,** 304–316 (2003).

48. Long, E. O., Sik Kim, H., Liu, D., Peterson, M. E. & Rajagopalan, S. Controlling Natural Killer Cell Responses: Integration of Signals for Activation and Inhibition. *Annu. Rev. Immunol.* **31,** 227–258 (2013).

49. Chan, C. J., Martinet, L. & Smyth, M. J. Molecular mechanisms of natural killer cell activation in response to cellular stress. *Cell Death Differ.* **21,** 5 (2013).

50. Biron, C. A. Activation and function of natural killer cell responses during viral infections. *Curr. Opin. Immunol.* **9,** 24–34 (1997).

51. Smyth, M. J., Hayakawa, Y., Takeda, K. & Yagita, H. New aspects of natural-killer-cell surveillance and therapy of cancer. *Nat. Rev. Cancer* **2,** 850–861 (2002).

52. Raulet, D. H., Gasser, S., Gowen, B. G., Deng, W. & Jung, H. Regulation of Ligands for the NKG2D Activating Receptor. *Annu. Rev. Immunol.* **31,** 413–441 (2013).

53. Timonen, T. & Saksela, E. Isolation of human NK cells by density gradient centrifugation. *J. Immunol. Methods* **36,** 285–291 (1980).

54. Vanherberghen, B. *et al.* Classification of human natural killer cells based on migration behavior and cytotoxic response. *Blood* **121,** 1326–1334 (2013).

55. Giannattasio, A. *et al.* Cytotoxicity and infiltration of human NK cells in in vivo-like tumor spheroids. *BMC Cancer* **15,** (2015).

56. Voskoboinik, I., Smyth, M. J. & Trapani, J. A. Perforin-mediated target-cell death and immune homeostasis. *Nat. Rev. Immunol.* **6,** 940–952 (2006).

57. Chowdhury, D. & Lieberman, J. Death by a Thousand Cuts: Granzyme Pathways of Programmed Cell Death. *Annu. Rev. Immunol.* **26,** 389–420 (2008).

58. Albeck, J. *et al.* Quantitative analysis of pathways controlling extrinsic apoptosis in single cells. *Mol. Cell* **30,** 11–25 (2008).

59. Lieberman, L. A. & Hunter, C. A. Regulatory pathways involved in the infection-induced production of IFN-gamma by NK cells. *Microbes Infect.* **4,** 1531–1538 (2002).

60. Christine A. Biron, Khuong B. Nguyen, Gary C. Pien, Leslie P. Cousens & Salazar-Mather, and T. P. NATURAL KILLER CELLS IN ANTIVIRAL DEFENSE: Function and Regulation by Innate Cytokines. *Annu. Rev. Immunol.* **17,** 189–220 (1999).

61. Mah, A. Y. & Cooper, M. A. Metabolic Regulation of Natural Killer Cell IFN-γ Production. *Crit. Rev. Immunol.* **36,** 131–147 (2016).

62. Natural killer cells are a source of interferon gamma that drives differentiation of CD4+ T cell subsets and induces early resistance to Leishmania major in mice. *J. Exp. Med.* **178,** 567–577 (1993).

63. Schroder, K., Hertzog, P. J., Ravasi, T. & Hume, D. A. Interferon-γ: an overview of signals, mechanisms and functions. *J. Leukoc. Biol.* **75,** 163–189

64. Cooper, M. A. *et al.* Human natural killer cells: a unique innate immunoregulatory role for the CD56bright subset. *Blood* **97,** 3146–3151 (2001).

65. Biron, C. A., Su, H. C. & Orange, J. S. Function and Regulation of Natural Killer (NK) Cells during Viral Infections: Characterization of Responsesin Vivo. *Methods* **9,** 379–393 (1996).

66. Orange, J. S. & Biron, C. A. An absolute and restricted requirement for IL-12 in natural killer cell IFN-gamma production and antiviral defense. Studies of natural killer and T cell responses in contrasting viral infections. *J. Immunol.* **156,** 1138–1142 (1996).

67. Orange, J. S., Wang, B., Terhorst, C. & Biron, C. A. Requirement for natural killer cell-produced interferon gamma in defense against murine cytomegalovirus infection and enhancement of this defense pathway by interleukin 12 administration. *J. Exp. Med.* **182,** 1045–1056 (1995).

68. Cerwenka, A. & Lanier, L. L. Natural killer cells, viruses and cancer. *Nat. Rev. Immunol.* **1,** 41 (2001).

69. Orange, J. S. Human natural killer cell deficiencies. *Curr. Opin. Allergy Clin. Immunol.* **6,** 399 (2006).

70. Ching, C. & Lopez, C. Natural Killing of Herpes Simplex Virus Type 1-Infected Target Cells: Normal Human Responses and Influence of Antiviral Antibody. *Infect. Immun.* **26,** 49–56 (1979).

71. Santoli, D., Trinchieri, G. & Lief, F. S. Cell-Mediated Cytotoxicity Against Virus-Infected Target Cells in Humans: I. Characterization of the Effector Lymphocyte. *J. Immunol.* **121,** 526–531 (1978).

72. Santoli, D., Trinchieri, G. & Koprowski, H. Cell-Mediated Cytotoxicity Against Virus-Infected Target Cells in Humans: II. Interferon Induction and Activation of Natural Killer Cells. *J. Immunol.* **121,** 532–538 (1978).

73. Godeny, E. K. & Gauntt, C. J. Involvement of natural killer cells in coxsackievirus B3-induced murine myocarditis. *J. Immunol.* **137,** 1695–1702 (1986).

74. Schmidt, S., Tramsen, L., Rais, B., Ullrich, E. & Lehrnbecher, T. Natural killer cells as a therapeutic tool for infectious diseases – current status and future perspectives. *Oncotarget* **9,** 20891–20907 (2018).

75. Terme, M., Ullrich, E., Delahaye, N. F., Chaput, N. & Zitvogel, L. Natural killer cell–directed therapies: moving from unexpected results to successful strategies. *Nat. Immunol.* **9,** 486–494 (2008).

76. Pietra, G. *et al.* Human natural killer cells: news in the therapy of solid tumors and high-risk leukemias. *Cancer Immunol. Immunother.* **65,** 465–476 (2016).

77. Dahlberg, C. I. M., Sarhan, D., Chrobok, M., Duru, A. D. & Alici, E. Natural Killer Cell-Based Therapies Targeting Cancer: Possible Strategies to Gain and Sustain Anti-Tumor Activity. *Front. Immunol.* **6,** (2015).

78. Childs, R. W. & Carlsten, M. Therapeutic approaches to enhance natural killer cell cytotoxicity against cancer: the force awakens. *Nat. Rev. Drug Discov.* **14,** 487–498 (2015).

79. Rabinovich, G. A., Gabrilovich, D. & Sotomayor, E. M. Immunosuppressive Strategies that are Mediated by Tumor Cells. *Annu. Rev. Immunol.* **25,** 267–296 (2007).

80. Garrido, F., Aptsiauri, N., Doorduijn, E. M., Garcia Lora, A. M. & van Hall, T. The urgent need to recover MHC class I in cancers for effective immunotherapy. *Curr. Opin. Immunol.* **39,** 44–51 (2016).

81. Burian, A. *et al.* HLA-F and MHC-I Open Conformers Bind Natural Killer Cell Ig-Like Receptor KIR3DS1. *PLOS ONE* **11,** e0163297 (2016).

82. Nausch, N. & Cerwenka, A. NKG2D ligands in tumor immunity. *Oncogene* **27,** 5944–5958 (2008).

83. Deng, W. *et al.* A shed NKG2D ligand that promotes natural killer cell activation and tumor rejection. *Science* **348,** 136–139 (2015).

84. López-Soto, A., Folgueras, A. R., Seto, E. & Gonzalez, S. HDAC3 represses the expression of NKG2D ligands ULBPs in epithelial tumour cells: potential implications for the immunosurveillance of cancer. *Oncogene* **28,** 2370 (2009).

85. Textor, S. *et al.* Human NK Cells Are Alerted to Induction of p53 in Cancer Cells by Upregulation of the NKG2D Ligands ULBP1 and ULBP2. *Cancer Res.* **71,** 5998–6009 (2011).

86. Li, H. *et al.* Pharmacological activation of p53 triggers anticancer innate immune response through induction of ULBP2. *Cell Cycle Georget. Tex* **10,** 3346–58 (2011).

87. Choy, J. C. *et al.* Granzyme B Induces Smooth Muscle Cell Apoptosis in the Absence of Perforin: Involvement of Extracellular Matrix Degradation. *Arterioscler. Thromb. Vasc. Biol.* **24,** 2245–2250 (2004).

88. Béziat, V. *et al.* Human NKG2A overrides NKG2C effector functions to prevent autoreactivity of NK cells. *Blood* **117,** 4394–4396 (2011).

89. Campbell, K. S. & Hasegawa, J. Natural killer cell biology: An update and future directions. *J. Allergy Clin. Immunol.* **132,** 536–544 (2013).

90. Moretta, A. *et al.* Activating receptors and coreceptors involved in human natural killer cell-mediated cytolysis. *Annu. Rev. Immunol.* **19,** 197–223 (2001).

91. Choi, P. J. & Mitchison, T. J. Imaging burst kinetics and spatial coordination during serial killing by single natural killer cells. *Proc. Natl. Acad. Sci.* **110,** 6488–6493 (2013).

92. Yamanaka, Y. J. *et al.* Single-cell analysis of the dynamics and functional outcomes of interactions between human natural killer cells and target cells. *Integr. Biol. Quant. Biosci. Nano Macro* **4,** 1175–1184 (2012).

93. Guldevall, K. *et al.* Imaging Immune Surveillance of Individual Natural Killer Cells Confined in Microwell Arrays. *PLOS ONE* **5,** e15453 (2010).

94. Zhang, Z., Guo, Y. & Feng, S.-S. Nanoimmunotherapy: application of nanotechnology for sustained and targeted delivery of antigens to dendritic cells. *Nanomed.* **7,** 1–4 (2011).

95. Khalil, D. N., Smith, E. L., Brentjens, R. J. & Wolchok, J. D. The future of cancer treatment: immunomodulation, CARs and combination immunotherapy. *Nat. Rev. Clin. Oncol.* **13,** 273–290 (2016).

96. Farkona, S., Diamandis, E. P. & Blasutig, I. M. Cancer immunotherapy: the beginning of the end of cancer? *BMC Med.* **14,** 73 (2016).

97. Coley, W. B. II. Contribution to the Knowledge of Sarcoma. *Ann. Surg.* **14,** 199–220 (1891).

98. McCarthy, E. F. The Toxins of William B. Coley and the Treatment of Bone and Soft-Tissue Sarcomas. *Iowa Orthop. J.* **26,** 154–158 (2006).

99. Matsueda, S. & Graham, D. Y. Immunotherapy in gastric cancer. *World J. Gastroenterol. WJG* **20,** 1657–1666 (2014).

100. Zitvogel, L., Ma, Y., Raoult, D., Kroemer, G. & Gajewski, T. F. The microbiome in cancer immunotherapy: Diagnostic tools and therapeutic strategies. *Science* **359,** 1366–1370 (2018).

101. June, C. H., O'Connor, R. S., Kawalekar, O. U., Ghassemi, S. & Milone, M. C. CAR T cell immunotherapy for human cancer. *Science* **359,** 1361–1365 (2018).

102. Sahin, U. & Türeci, Ö. Personalized vaccines for cancer immunotherapy. *Science* **359,** 1355–1360 (2018).

103. Ribas, A. & Wolchok, J. D. Cancer immunotherapy using checkpoint blockade. *Science* **359,** 1350–1355 (2018).

104. Han, J. *et al.* CAR-Engineered NK Cells Targeting Wild-Type EGFR and EGFRvIII Enhance Killing of Glioblastoma and Patient-Derived Glioblastoma Stem Cells. *Sci. Rep.* **5,** 11483 (2015).

105. Beldi-Ferchiou, A. & Caillat-Zucman, S. Control of NK Cell Activation by Immune Checkpoint Molecules. *Int. J. Mol. Sci.* **18,** 2129 (2017).

106. Tam, Y. k. *et al.* Characterization of Genetically Altered, Interleukin 2-Independent Natural Killer Cell Lines Suitable for Adoptive Cellular Immunotherapy. *Hum. Gene Ther.* **10,** 1359–1373 (1999).

107. Gong, J. H., Maki, G. & Klingemann, H. G. Characterization of a human cell line (NK-92) with phenotypical and functional characteristics of activated natural killer cells. *Leukemia* **8,** 652–658 (1994).

108. Klingemann, H. G. & Miyagawa, B. Purging of malignant cells from blood after short ex vivo incubation with NK-92 cells [letter; comment]. *Blood* **87,** 4913–4914 (1996).

109. Choi, P. J. & Mitchison, T. J. Quantitative analysis of resistance to natural killer attacks reveals stepwise killing kinetics. *Integr. Biol.* **6,** 1153–1161 (2014).

110. Tonn, T., Becker, S., Esser, R., Schwabe, D. & Seifried, E. Cellular Immunotherapy of Malignancies Using the Clonal Natural Killer Cell Line NK-92. *J. Hematother. Stem Cell Res.* **10,** 535–544 (2001).

111. Suck, G. *et al.* NK-92: an 'off-the-shelf therapeutic' for adoptive natural killer cell-based cancer immunotherapy. *Cancer Immunol. Immunother. CII* **65,** 485 (2016).

112. Sánchez-Madrid, F. & del Pozo, M. A. Leukocyte polarization in cell migration and immune interactions. *EMBO J.* **18,** 501–511 (1999).

113. Vyas, Y. M., Maniar, H. & Dupont, B. Visualization of signaling pathways and cortical cytoskeleton in cytolytic and noncytolytic natural killer cell immune synapses. *Immunol. Rev.* **189,** 161–178 (2002).

114. Medvedev, A. E. *et al.* Regulation of Fas and Fas-ligand expression in NK cells by cytokines and the involvement of Fas-ligand in NK/LAK cell-mediated cytotoxicity. *Cytokine* **9,** 394–404 (1997).

115. Wang, R., Jaw, J. J., Stutzman, N. C., Zou, Z. & Sun, P. D. Natural killer cell-produced IFN-γ and TNF-α induce target cell cytolysis through up-regulation of ICAM-1. *J. Leukoc. Biol.* **91,** 299–309 (2012).

116. Caron, G. *et al.* Human NK cells constitutively express membrane TNF-alpha (mTNFalpha) and present mTNFalpha-dependent cytotoxic activity. *Eur. J. Immunol.* **29,** 3588–3595 (1999).

117. Salcedo, T. W., Azzoni, L., Wolf, S. F. & Perussia, B. Modulation of perforin and granzyme messenger RNA expression in human natural killer cells. *J. Immunol.* **151,** 2511–2520 (1993).

118. Champsaur, M. & Lanier, L. L. Effect of NKG2D ligand expression on host immune responses. *Immunol. Rev.* **235,** 267–285 (2010).

119. Xiao, S. *et al.* FasL promoter activation by IL-2 through SP1 and NFAT but not Egr-2 and Egr-3. *Eur. J. Immunol.* **29,** 3456–3465 (1999).

120. Sachs, N. & Clevers, H. Organoid cultures for the analysis of cancer phenotypes. *Curr. Opin. Genet. Dev.* **24,** 68–73 (2014).

121. Bartfeld, S. *et al.* In Vitro Expansion of Human Gastric Epithelial Stem Cells and Their Responses to Bacterial Infection. *Gastroenterology* **148,** 126-136.e6 (2015).

122. Drost, J. & Clevers, H. Organoids in cancer research. *Nat. Rev. Cancer* **18,** 407–418 (2018).

123. Mata, A., Fleischman, A. J. & Roy, S. Characterization of Polydimethylsiloxane (PDMS) Properties for Biomedical Micro/Nanosystems. *Biomed. Microdevices* **7,** 281–293 (2005).

124. Hsieh, C.-H., Huang, C.-J. C. & Huang, Y.-Y. Patterned PDMS based cell array system: a novel method for fast cell array fabrication. *Biomed. Microdevices* **12,** 897–905 (2010).

125. Olofsson, P. E. *et al.* ~Distinct Migration and Contact Dynamics of Resting and IL-2-Activated Human Natural Killer Cells. *Front. Immunol.* **5,** (2014).

126. Forslund, E. *et al.* Microchip-Based Single-Cell Imaging Reveals That CD56dimCD57-KIR-NKG2A+ NK Cells Have More Dynamic Migration Associated

with Increased Target Cell Conjugation and Probability of Killing Compared to CD56dimCD57-KIR-NKG2A- NK Cells. *J. Immunol. Baltim. Md 1950* **195,** 3374–3381 (2015).

127. E. Christakou, A., Ohlin, M., Önfelt, B. & Wiklund, M. Ultrasonic three-dimensional on-chip cell culture for dynamic studies of tumor immune surveillance by natural killer cells. *Lab. Chip* **15,** 3222–3231 (2015).

128. Xu, Y., Zhou, S., Lam, Y. W. & Pang, S. W. Dynamics of Natural Killer Cells Cytotoxicity in Microwell Arrays with Connecting Channels. *Front. Immunol.* **8,** (2017).

129. Holmes, T. D. *et al.* A Human NK Cell Activation/Inhibition Threshold Allows Small Changes in the Target Cell Surface Phenotype To Dramatically Alter Susceptibility to NK Cells. *J. Immunol.* **186,** 1538–1545 (2011).

130. Smyth, M. J. *et al.* NKG2D function protects the host from tumor initiation. *J. Exp. Med.* **202,** 583–588 (2005).

List of Publications

1. Choi M, Shi J, **Zhu Y**, Yang R, Cho K. (2017) Network dynamics-based stratification of cancer panel for systemic prediction of anticancer drug response. Nature Communications, 8:1940.
2. Kueh HY, **Zhu Y**, Shi J. (2016) A simplified Bcl-2 network model reveals quantitative determinants of cell-to-cell variation in sensitivity to anti-mitotic chemotherapeutics. Scientific Reports, 6: 36585.
3. **Zhu Y**, Huang B, Shi J. (2016) Fas ligand and lytic granule differentially control cytotoxic dynamics of Natural Killer cell against cancer target. Oncotarget. 7(30):47163-72.
4. **Zhu Y**, Zhou Y, Shi J. (2014) Post-slippage multinucleation renders cytotoxic variation in anti-mitotic drugs that target the microtubules or mitotic spindle. Cell Cycle. 13(11):1756-64.
5. Wong CC, Tse AP, Huang YP, **Zhu Y**, Chiu DK, Lai RK, Au SL, Kai AK, Lee JM, Wei LL, Tsang FH, Lo RC, Shi J, Zheng YP, Wong CM, Ng IO. (2014) Lysyl oxidase-like 2 is critical to tumor microenvironment and metastatic niche formation in hepatocellular carcinoma. Hepatology. 60 (5):1645-1658.
6. Liang J, Mok AW, **Zhu Y**, Shi J. (2013) Resonance versus linear responses to alternating electric fields induce mechanistically distinct mammalian cell death. Bioelectrochemistry. 94C: 61-68.

CURRICULUM VITAE

Academic qualifications of the thesis author, Ms. ZHU Yanting:

- Received the degree of Bachelor of Pharmacy (Hons) in Chinese Medicine from Hong Kong Baptist University, November 2011.
- Received the degree of Master of Philosophy from Hong Kong Baptist University, November 2014.

August 2018